

Review

Nanocomposite-Based Electrochemical Sensors for Neurotransmitters Detection in Neurodegenerative Diseases

Thenmozhi Rajarathinam ¹, Mijeong Kang ¹, Sungmoo Hong ² and Seung-Cheol Chang ^{1,*} 

¹ Department of Cogno-Mechatronics Engineering, College of Nanoscience and Nanotechnology, Pusan National University, Busan 46241, Republic of Korea

² Interdisciplinary Department for Innovative Manufacturing Engineering, Pusan National University, Busan 46241, Republic of Korea

* Correspondence: s.c.chang@pusan.ac.kr

Abstract: Neurotransmitters (NTs) are crucial regulatory molecules responsible for maintaining the neurophysiological functioning of the brain. Dysregulated levels of certain NTs, such as dopamine, serotonin, norepinephrine, epinephrine, glutamate, and gamma-aminobutyric acid, are often correlated with the pathogenesis of neurodegenerative diseases that involve the progressive and selective loss of structure or function of neuronal systems. Therefore, the identification and validation of relevant biomarkers are essential to diagnose these diseases much earlier. However, the quantitative analysis of NTs is challenging because of their dynamic release and presence of low concentrations. Accordingly, nanocomposite (NC)-based electrochemical sensors have been studied extensively and are gaining tremendous interest due to their high sensitivity, response rate, stability, portability, ease of use in point-of-care diagnostics, amenability to microprocessing, and low cost. In this review, we first briefly discuss the potential biomarkers of neurodegenerative diseases, NC-based electrochemical sensors and their advantages and disadvantages, and the properties of the NCs, which further increase the sensor performance. Finally, we summarized the future perspectives of NC-based electrochemical sensors in the clinical set-up for NTs detection to identify research gaps.

Keywords: neurotransmitters; neurodegenerative diseases; nanocomposite; electrochemical sensors; point-of-care diagnostics



Citation: Rajarathinam, T.; Kang, M.; Hong, S.; Chang, S.-C.

Nanocomposite-Based Electrochemical Sensors for Neurotransmitters Detection in Neurodegenerative Diseases.

Chemosensors **2023**, *11*, 103.
<https://doi.org/10.3390/chemosensors11020103>

Academic Editor: Gabriela Broncová

Received: 4 January 2023

Revised: 21 January 2023

Accepted: 28 January 2023

Published: 1 February 2023



Copyright: © 2023 by the authors. Licensee MDPI, Basel, Switzerland. This article is an open access article distributed under the terms and conditions of the Creative Commons Attribution (CC BY) license (<https://creativecommons.org/licenses/by/4.0/>).

1. Introduction

The human brain is a complex part that consists of various neurotransmitters (NTs) responsible for neurotransmission. NTs play vital roles in brain functioning, and changes in NT concentrations have been correlated with various neurodegenerative diseases (NDs). NDs encompass a large category of diseases with different pathological patterns and clinical presentations, such as Alzheimer's disease (AD), Parkinson's disease (PD), and Huntington's disease (HD). NDs affect millions of people worldwide, and their incidence increases with age [1–4]. Real-time detection of NTs is significant in neuroscience as it contributes to the clinical diagnosis of NDs. Since NTs levels are very low in the picomolar/nanomolar ranges, a high concentration of ascorbic acid (AA), 200–500 μM in the biological samples, is the main challenge in NTs monitoring. Also, the peak overlaps between NTs, such as epinephrine (EP), dopamine (DA), and norepinephrine (NE), occur due to their chemical structure similarities, often resulting in electro-oxidation at the same applied potential. However, selective electrochemical detection of neurotransmitters is a main challenge in biological samples. Despite these drawbacks, world-wide efforts have contributed to the development of cost-effective electrochemical sensors with improved sensitivity, selectivity, response rate, and stability properties [5,6]. For electrochemical sensors fabrication, various advanced technologies such as molecular imprinting, screen printing, laser-based nanostructuring including 3D printing, etc. have been employed. Of these, molecular imprinting and screen printing are widely used and are commendable for producing high-performance sensors [5].

Among NTs, DA functions as both excitatory and inhibitory neurotransmitters, whereas gamma-aminobutyric acid (GABA) and serotonin (5-HT) function as inhibitory neurotransmitters crucial in reducing neuronal excitability throughout the brain. In contrast, glutamate (GLU), EP, and NE are the primary excitatory neurotransmitters that induce neuronal excitability and damage. Dysregulated levels of these biomarkers have been reported in several NDs and psychiatric disorders, including epilepsy, AD, PD, HD, ALS disease, schizophrenia, alcoholism, and stroke. Thus, monitoring these NTs release is ideal for diagnosing NDs, as it enables the understanding of neural functions and plasticities in the brain [7].

Conventionally, NTs are measurable using high-performance liquid chromatography (HPLC) and capillary electrophoresis separations [8], and mass spectroscopy [9,10]. Although these techniques enable analyte detection, they are not suited for point-of-care diagnostics owing to several disadvantages, such as the requirement of a large sample volume, time consumption, expensiveness, laborious sample preparation, and poor sensitivity [11]. If improved sampling methods with better spatial resolution and recovery were possible, these methods would have been proven practically easy [10]. Typically, neurons communicate via synapses that are formed between neurons after their exocytotic release into the extracellular space. The released NTs estimation remains a big challenge to conventional analytical techniques because of their fast release and clearance, low concentrations, and the presence of other common analytes [10]. In this regard, electrochemical sensors are viable substitutes as they outweigh these disadvantages and are highly applicable in clinical scenarios because of their high sensitivity, easy miniaturization, portability, cost-effectiveness, stability, and reliability [12].

The integration of nanocomposites (NCs) in the electrochemical sensors substantially improves the surface-to-volume ratio, high specific surface area [6], quick electron transfer, much lower surface fouling, and low background currents [13]. Nonetheless, the overpotential and low current responses, are considered as analytical challenges for the determination of NT. These problems can be easily resolved by modifying the electrodes with a variety of conductive NCs. So far, several strategies have been employed to maximize the sensor selectivity. For example, strategies include surface functionalization/doping by metals; designing NCs with heterostructures, such as hierarchical metal oxides and binary metal oxides; utilization of permselective membranes, such as Nafion, chitosan, poly(*o*-phenylenediamine) as interference-rejecting layer, etc. [6]. Therefore, NCs have significant potential for easy fabrication of enzyme-free, stable, and sensitive electrochemical sensors for NTs detection [14]. Even though various enzymatic biosensors have already shown effective detection of NTs, their poor sensitivity due to indirect electron-transfer mechanisms poses a challenge [15]. NC-modified electrochemical sensors could rectify these problems, fulfilling the detection requirements. Therefore, many researchers have focused on making diagnoses more effective and more prompt at molecular and cellular levels by applying electrochemical sensors. In this context, from the year 2018 to 2022, more than 250 publications are available for the NC-based electrochemical sensors, while less than 20 publications are available for the NTs measurable NC-based electrochemical sensors (Figure 1) [16].

Recently, carbon- and polymer-based NCs, molecularly imprinted polymers (MIPs), metal-organic frameworks (MOFs), and metal- (Pt, Au, Pd, Ni, Cu, Co, Mn, Zn) and metal oxide-based NCs oxides (NiO, CuO, Cu₂O, Co₃O₄, MnO₂, ZnO) have been used as promising electrode modifiers because they further enhance the sensitivity and dynamic range of detection. Apart from these, monometallic nanoparticles (such as Pt, Au, Pd), bi-metallic alloys (Pt–Pb, Pt–Ru, Pt–Au, etc.), mixed metal oxides [17], metal dichalcogenides [18], transition metal oxides and their hybrid nanostructures were reported to enhance the sensitivity and selectivity of the sensors. This excellent electrocatalytic activity of the NCs holds a promising future for the design and implementation of electrochemical sensors with enhanced sensitivity [19,20]. The motivation of this review article is to emphasize the diagnostic biomarkers of NDs, advancements made in NCs to develop sensors for NTs, and their properties responsible for enhanced sensitivity and fast-response characteristics.

The NCs' sensing mechanisms, strengths, and limitations of NTs' targeted electrochemical sensors are also highlighted. Also, this review article includes a summary of the currently emerging electrochemical techniques for real-time NTs detection, followed by a conclusion and future perspectives. We have focused mainly on amperometric and voltammetric sensors that are fabricated using carbon-based electrodes, such as carbon paste (CPE), glassy carbon (GCE), screen-printed carbon (SPCE), and molecular imprinted electrodes (MIPs) with an exemption of laser nanopatterned electrodes.

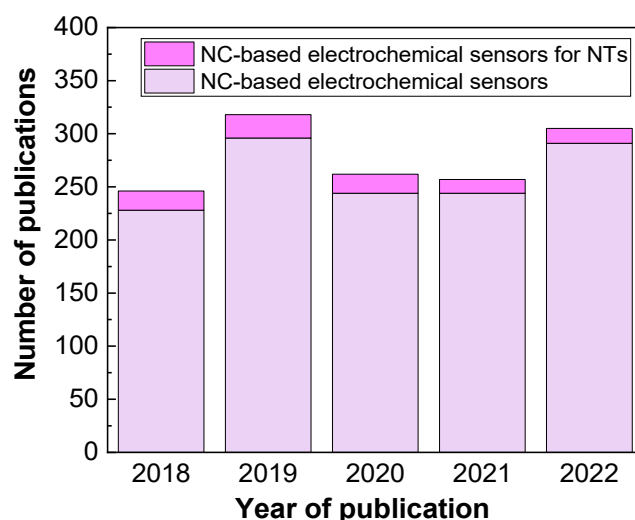


Figure 1. Annual trend in the number of publications for “NC-based electrochemical sensors” (light violet) and “NC-based electrochemical sensors for NTs” (magenta) from 2018 to 2022. Database: PubMed®.

2. Diagnostic Biomarkers of NDs

Based on their function, NTs are categorized as inhibitory (GABA and 5-HT), excitatory (glutamate, EP, and NE), or both (DA). Among these NTs, DA, chemically known as 3,4-dihydroxyphenethylamine, is primarily synthesized in several brain areas, including the substantia nigra and ventral tegmental area. Additionally, DA is synthesized in the medulla of the adrenal glands. Schizophrenia, with manifestations such as perception disturbances and hallucinations, occurs due to imbalanced DA levels in the brain. Besides schizophrenia, neurological/motor diseases, including PD, are also linked to decreasing DA levels [21]. Another inhibitory NT, GABA, synthesized from GLU, is predominantly found in the brain. GABA acts as a regulator in the growth, proliferation, migration, and differentiation of neurons. GABA causes hyperpolarization, which is induced by potassium ion efflux or influx into the neuronal cells. GABA signaling dysregulation has been linked to neurological conditions such as epilepsy, PDs, and HDs [22]. Chemically known as 5-hydroxytryptamine or serotonin, 5-HT is an important inhibitory NT that is principally stored in serotonergic neurons. Altered 5-HT levels affect muscle contraction and endocrine regulation, leading to anxiety and depression [23].

Among excitatory NTs, GLU is an important NT at normal levels, with a large array of normal physiological functions, including memory, cognition, and mood regulation. Glutamine is then transported back to neurons, where it is reconverted to glutamate [24]. However, dysregulated GLU levels cause hyperexcitability in postsynaptic neurons, leading to GLU-induced excitotoxic conditions in AD, HD, and diffused brain injuries [25,26]. EP and NE are excitatory NTs secreted by the adrenal medulla and released into the blood circulation. As important excitatory NTs, both EP and NE play vital roles in human health, preparing for the fight or flight reactions [27]. Generally, EP exists as large organic cations in nervous tissues and body fluids [28]. In humans, the normal concentrations of DA, NE, and EP are 195.8, 10,048.7 and 764.3 pM, respectively. The normal 5-HT and GLU concentrations in the brain are 1.14 μ M and 2.0 μ M, respectively. The much-increased concentration levels may contribute to NDs [29,30].

3. Sensitive Nanocomposite Materials

NCs, including carbon, polymer, metal, metal oxide, and other types of engineered NCs, are considered outstanding electrode modifiers for NTs detection. Of these, carbon-based nanomaterials provide excellent electrocatalytic platforms for the sensitive detection of NTs. Carbon-based nanomaterials, including hierarchical 3D porous carbon, graphene, and carbon nanotube-based NCs, are critical in the future development of advanced point-of-care diagnostics [31].

3.1. Carbon-Based NCs

Hierarchical porous carbon materials consist of distinct pore diameters. Especially, macropores enhance diffusion, mesopores promote mass transfer, and micropores increase the specific surface area, thus boosting the sensing performances. The evolution of such pores in the material enables superior electrochemical properties with high sensitivity, and repeatability, thereby preventing surface fouling [32]. Dong et al. synthesized NC-based hierarchical porous carbon with distinct mesopores and macropores to construct a DA sensor. The NC has enabled increased active sites, faster electron transfer rates, and better electrochemical properties toward DA detection [33]. Similarly, Liu et al. has designed a sensor modified with mesoporous carbon, demonstrating excellent sensitivity and selectivity for DA sensing [34]. Because the three-dimensional porous carbon possesses a high sp^2 content, it ensures DA detection with a linear range between 800 nM–400 μ M with a lower limit of detection (LOD) of 100 nM and showed better anti-interference properties amidst common interfering substances [32].

In addition to the distinctive sheet-like structure of graphene, three-dimensional graphene aerogels have large specific surface area and pore volume. High-porosity graphene aerogels with connected networks have been designed to further improve the electrochemical performance of sensors [35]. An amperometric sensor based on graphene and macroporous carbon aerogels was constructed to estimate the DA in serum samples. The sensor elicited a fast response time, good repeatability, high sensitivity, and selectivity for DA amongst high concentrations of ascorbic acid (AA) and uric acid (UA). To verify the accuracy of the sensor for DA determination, the results were validated via chromatographic analysis [36]. Using a simple physical adsorption technique, a three-dimensional reduced graphene oxide (rGO)/polyurethane porous NC with connected pores was developed. Differential pulse voltammetry (DPV) using the rGO/polyurethane NCs against DA exhibited a linear response range of 100–1150 pM, with a LOD of 1 pM for DA. This sensor is used for the selective screening of DA, but the influence of other interferents such as NE has not been studied [37].

Graphene shows minimal charge-transfer resistance and enhanced electrochemical activity owing to its large potential window for fast electron transfer rates. The sensing mechanism of graphene is based on the direct electron transfer processes, which are predominantly diffusion-controlled. The factor that plays a key role in electron transfer at the graphene surface is the nature of the analyte (electron donor or acceptor). For graphene-based NCs, the Schottky junctions formed between graphene and metal oxides are proven beneficial for electron transfer. In graphene/metal oxides NCs, the high conductivity of graphene and sensitivity of metal oxides manifest enhanced sensing performances [17]. Therefore, graphene and its derivatives are pertinent for the design of electrochemical sensors to study NDs [38].

Suriyaprakash et al. synthesized p-aminophenol-functionalized rGO using a one-step approach to develop an electrochemical sensor with a sensing ability of 7.5 nM for DA (Figure 2A) [39]. Another study involving graphene oxide (GO) nanoribbon/poly(diallyldimethylammonium chloride)/gold nanoparticle (AuNP)-based NCs was conducted by Liu et al. for DA detection [40]. The electron transfer is enabled by the π - π interaction between the phenyl moiety of DA and the π conjugated graphene [41,42]. The electrocatalytic activity of the P-doped graphene was sufficient for DA oxidation. AuNP loadings onto the P-doped graphene have improved DA sensing performance with a linear

range from 0.1 to 180 μM and a LOD of 0.002 μM (Figure 2B) [43]. Self-rolled TiO_2 microscroll/graphene NCs were developed for real-time DA-sensing applications. Rolled-up nanomembranes enable mixed electron/ion conductive networks, which serve as supportive layers for the continuous transport of electrons [44]. A carbon paste electrode (CPE) modified with GO/co-polymer was used for EP electro-oxidation. The LOD was 0.65 μM with the linear range being 1.5–600.0 μM using the DPV technique. The sensor could simultaneously detect EP and DA in human serum samples and measure EP in drug samples, manifesting successful recoveries [45]. Graphene modified Pd sensor was formulated to measure NE in pharmaceutical and human urine samples. The sensor exhibited enhanced peak currents with a sensitivity of 0.0174 $\mu\text{A mM}^{-1}$ and a LOD of 67.44 nM for NE. The delocalized π -electron clouds of graphene enable sufficient electron transport to and from the electrode. The increased surface area of graphene and the conductive properties of Pd promote strong affinity toward the target NE molecules [46].

Ma et al. applied a Cu-ion chelation-assisted chitosan (CS)-derived carbon foam-based sensor for GLU detection. The chelation process between Cu and the target GLU enables easy chronoamperometric (CA) detection via redox reactions [47]. A non-enzymatic sensor for gamma-aminobutyric acid (GABA) neurotransmitter was designed utilizing GO/Au electrodes modified with orthophthalaldehyde and alkylthiol ligands to interact with the target GABA in human serum and urine matrices. A LOD of approximately 98 nM was attained and is sufficient to detect GABA in human samples (Figure 3) [48]. However, only a few electrochemical sensors are available to date for GLU and GABA detection.

Graphene quantum dots (GQDs) are a zero-dimensional nanomaterial with a thickness of less than ten layers [49]. GQDs have small size, high surface area, chemical inertness, good dispersibility, low toxicity, and electrical and chemical properties [50]. Due to these attractive properties, GQDs are advantageous for the electrochemical detection of various analytes. The possibility of π - π interaction with the analyte enables facile electron-transfer. These electronic features of GQDs minimize the likelihood of passivation between sensing layers [17]. Pang et al. employed GQDs for the selective detection of DA, taking advantage of the negative carboxyl groups that could electrostatically interact with the amine groups in DA [51]. Luhana et al. constructed a sensor utilizing cobalt phthalocyanine onto amine functionalized GQDs for detecting catecholamines in calf serum samples. The LODs of 0.20 μM (DA), 0.45 μM (NE), and 0.23 μM (EP) were attained using the sensor without any interferences from AA [52]. GQDs-multiwalled carbon nanotubes (MWCNTs) NCs-modified sensor was fabricated to detect DA with a LOD of 0.87 nM, which was then applied in human serum and living pheochromocytoma (PC12) cells to evaluate the DA levels [53]. GQDs sized 1–5 nm were combined with acid-functionalized MWCNTs to construct a DA sensor, which exhibited a linearity from 0.25–250 μM with a LOD of 95 nM. The developed sensor interacted selectively with DA amidst glucose, KCl, ascorbic acid, and GLU molecules. DA detection ability in human serum was also analyzed, and this property is attributable to the surface coverage, signal enhancement, and electrocatalytic activity of the GQD/MWCNTs NCs [54].

Carbon nanotubes (CNTs) are molecular-scale wires with special characteristics, including high conductivity, anti-fouling capability, and high surface area. These characteristics enhance the electron transfer processes [55]. The π -electrons in the CNT tube ends are responsible for the high-response current and mass-transfer coefficient. Their orbital structure exhibits sp^2 hybridization of carbon atoms, which aids in the easy flow of electrons [56]. The length of the CNTs also contributes to the electron transfer rate. CNTs are highly intriguing for the sensor design because of their electrical conductivity, resembling that of Cu. Single-walled CNTs (SWCNTs) are one-dimensional materials with enriched electrons on the surface. MWCNTs comprise several to tens of graphitic shells with a minimal layer spacing. Each carbon layer in MWCNTs has a unique chirality and electronic property resulting in a complex structure [57].

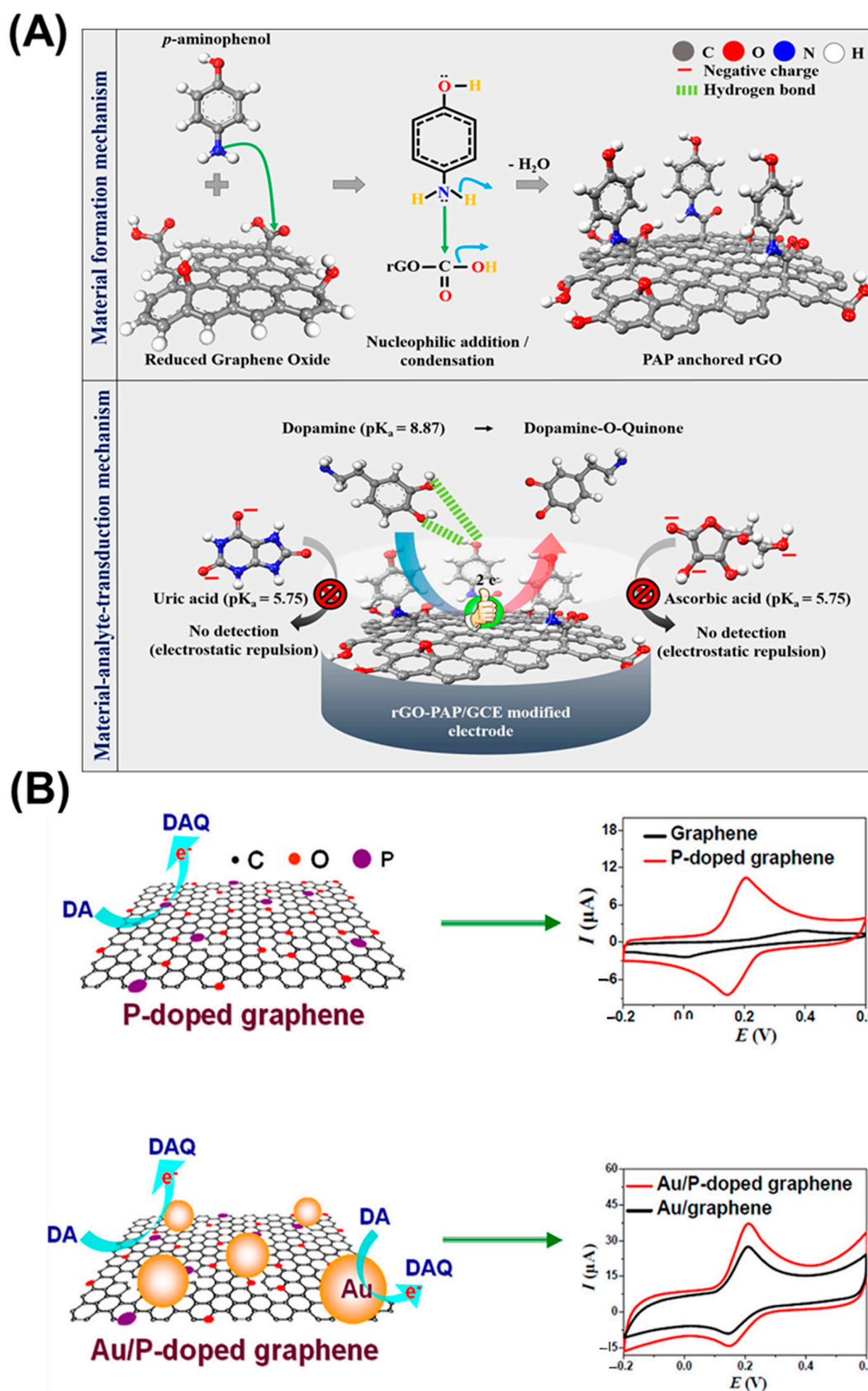


Figure 2. Schematic of the electrochemical sensor based on (A) rGO and (B) graphene NCs and their interactions with DA neurotransmitter. Reprinted with permission from refs. [39,43]. Copyright 2021, American Chemical Society and Copyright 2018, Springer.

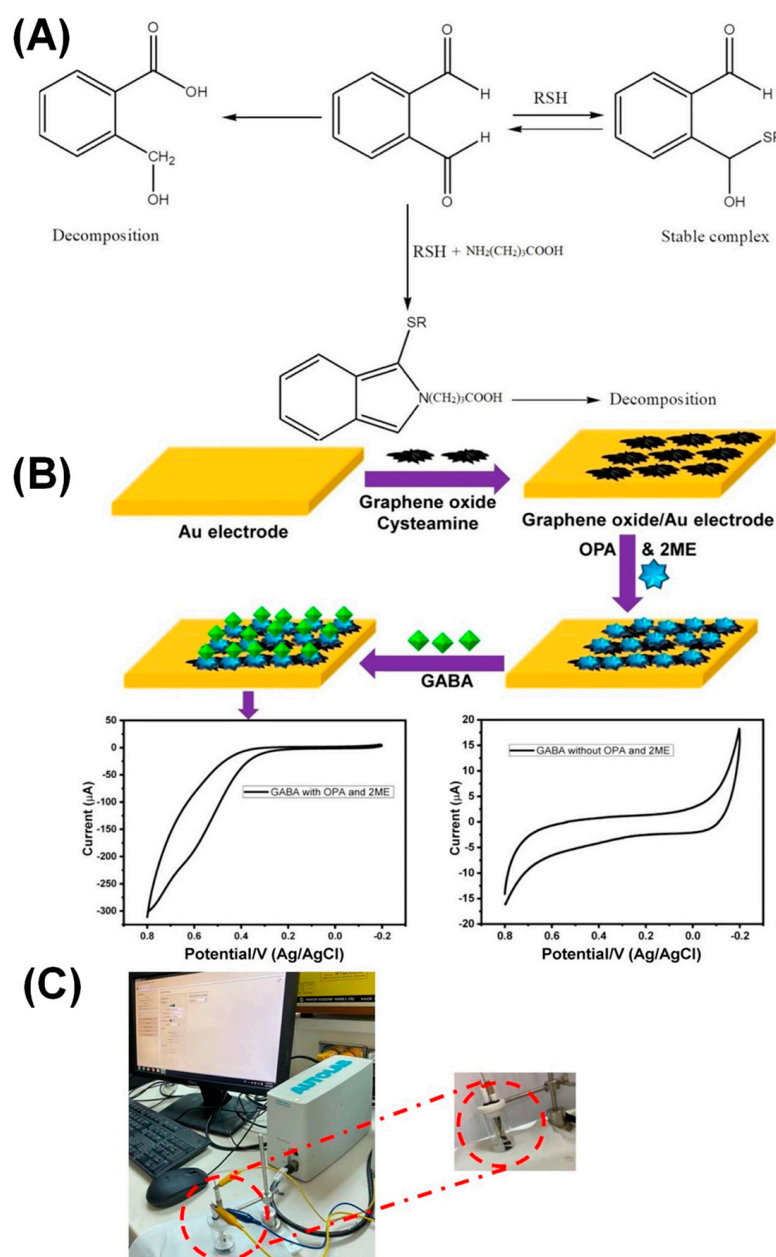


Figure 3. (A) Illustration of the interaction between GABA and the ligands. (B) Schematic of the GABA sensor. (C) Photographs of the graphene oxide-modified Au sensor. Reprinted with permission from ref. [48]. Copyright 2020, Elsevier.

Chapin et al. designed cell culture systems integrated with Au-SWCNT-modified sensors that could detect 5-HT to study the gut-brain axis signaling processes. The sensor drop coated with SWCNTs demonstrated a sensitivity of $4.5 \mu\text{A}/\mu\text{M}$, with a 100 nM – $1 \mu\text{M}$ linear range, which could target much lower 5-HT concentrations with a low-time resolution. The sensor demonstrated a transition from diffusion-controlled to adsorption-controlled behavior, indicating an increased 5-HT binding. This property of the sensor arises from the SWCNT film [58]. In another study, SWCNTs were de-bundled in a polymeric dispersant consisting of a copolymer of polystyrene sulfonate and methacrylate of lipoic acid to fabricate a disposable sensor for NE. The sensor exhibited a wide linear range (100 nM – $2.0 \mu\text{M}$) and a LOD of 62.0 nM . The sensor was then applied to ex vivo rat tissue samples, such as the adrenal gland and brain (locus coeruleus) tissues, to quantify NE levels [59].

A platinum (Pt)-MWCNTs NC-modified SPCE was prepared to monitor DA released from PC 12 cells after K^+ stimulation. An ultralow LOD of 2 nM was achievable for DA, and this sensor was useful for monitoring extracellular DA levels (Figure 4) [60]. The gold electrode was modified using MWCNTs for the simultaneous estimation of catecholamines in mouse brain and human urine samples [61]. Electrospun polymer nanofibers with MWCNTs were used to detect DA, with a LOD of 0.15 μ M [62]. MWCNTs functionalized with MoS_2 were applied to detect EP with the LOD of 3.0 μ M in water samples. Along with MWCNTs, two-dimensional MoS_2 nanostructures provide enhanced electrocatalytic activity for ultrasensitive EP detection [63]. CS-functionalized MWCNTs were used for the selective voltammetric detection of EP against significant electroactive interferences in artificial urine and adrenaline formulations [64]. The MWCNT-ionic liquid crystal and crown ether NC were modified on the GCE to selectively detect 5-HT in human serum samples. The large surface area of MWCNTs promotes stable host-guest complexes between crown ether NC and 5-HT [65].

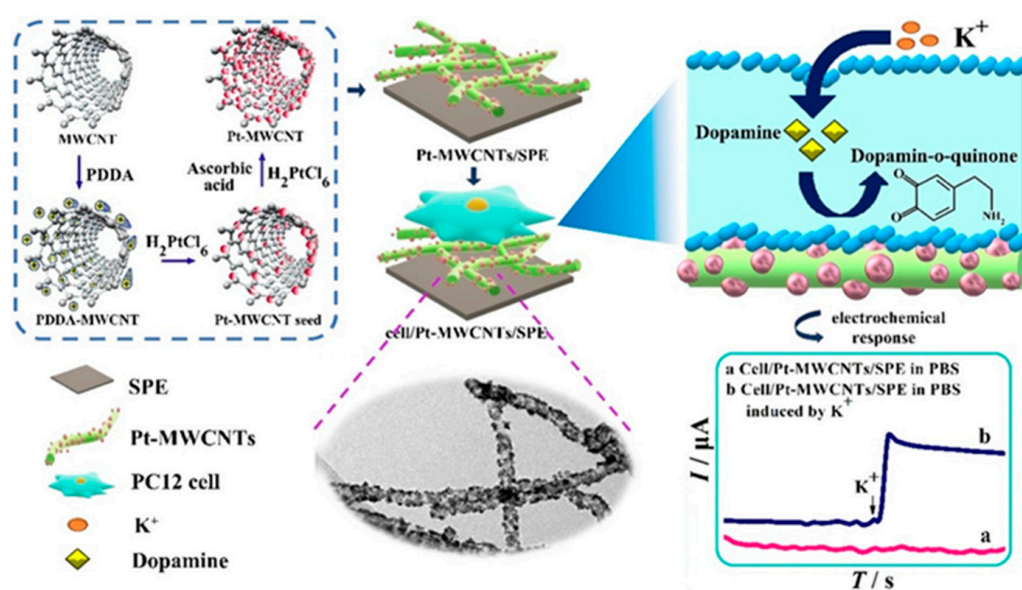


Figure 4. Schematic of the electrochemical sensor (Pt-MWCNTs/SPCE) for monitoring DA release from rat pheochromocytoma (PC-12) cells. Reprinted with permission from ref. [60]. Copyright 2020, Elsevier.

Highly compressed MWCNTs carbon-epoxy-based sensors have been used for 5-HT estimation. Although epoxy is a non-conducting polymer, it has been incorporated to increase the sensor structural stability. The enhanced electroanalytical performance of the sensor was due to the high compression of the MWCNTs. As 5-HT oxidative products are known to cause fouling, the sensor was analyzed to evaluate the extent of electrode fouling using a redox probe. The sensor also demonstrated decreased internal resistance and increased capacitance owing to the highly compressed MWCNTs [66]. Similarly, acid-activated MWCNTs and poly(3, 4-ethylene dioxythiophene) (PEDOT) were modified on a pencil graphite electrode (PGE) for electrochemical sensing of 5-HT. The sensor showed a LOD of 0.092 μ M, and human serum sample recovery rates were satisfactory, proving the reliability in 5-HT detection. Owing to the presence of acid-activated MWCNTs, the peak currents in cyclic voltammetry (CV) were increased by fifteen times, and in DPV, the peak current was found increased by eight times. In addition, the affinity for 5-HT was higher in the acid-activated MWCNT/PEDOT/PGE than in bare PGE, signifying high sensitivity of the modified sensor [67].

An electrochemical sensor utilizing poly (diallyl dimethylammonium) chloride-rGO-MWCNT was formulated to detect dual analytes, DA, and 5-HT. DPV exhibited a linear range of 0.05–120.0 μ M and 05–50.0 μ M with a LOD of 0.016 μ M and 0.0098 μ M for DA and 5-HT, respectively. The combined carbon nanomaterials (MWCNT and rGO) exhibited

excellent electrical conductivity. Positively charged poly (diallyl dimethylammonium) chloride has contributed to the dispersibility of rGO. The combined advantages of these NCs have enabled the simultaneous quantification of DA and 5-HT in rat plasma samples [68]. Similarly, in another study, carbon electrodes with graphene-like characteristics (electrochemically treated MWCNT hybrids with fused and unzipped morphologies) were modified over a GCE to detect both DA and 5-HT. The performance enhancement of the sensor, that is, the peak separation capability, was greater than 130 mV between DA and 5HT. Moreover, the conductivity of the sensor is highly commendable [69].

Voltammetric techniques using highly densified CNT fiber microelectrodes were employed to evaluate DA, 5-HT, EP, and NE levels. LOD of approximately 32, 31, 64, and 9 pM were obtained for DA, 5-HT, EP, and NE, respectively. Picomolar levels of DA can be detected in human biological fluids and living PC12 cells [70]. Similarly, CNT-yarn microelectrodes were employed as electrode modifiers to detect 5-HT and DA in artificial cerebral fluid through fast-scan cyclic voltammetry (FSCV) experiments [71]. CNT-based microelectrode arrays were used to detect DA (LOD of 7 nM). As microelectrode arrays are suitable devices for multisite detection, DA release from neural tissues can be measured. Because these CNT-based microelectrodes promote faster electron transfer kinetics, lower LODs, increased resolution, and increased current responses, they are employed for real-time measurements of NTs [72].

3.2. Polymer-Based NCs

Conducting polymers are crystalline and contain polyconjugated chains of alternating single (σ) and double (π) bonds that are highly reactive to molecular interactions, providing excellent signal transduction for target detection. The solubility and processability of polymers are based on the attached side chains, and dopants that impart mechanical, electrical, and optical properties [73]. Conducting polymers have several advantages as electron transfer mediators. Formation of a protective polymer layer and tailoring the thickness of polymer layer are known to increase the electroactivity of the sensing area. Selectivity toward the target can be improvised by the tethering of specific functional groups in the polymer structures [74].

Among conducting polymers, polyaniline (PANI) is exemplary because it is redox-active, conductive in neutral pH solutions, stable, and easy to fabricate. Graphite screen-printed electrodes electrodeposited with PANI and AuNPs were used to fabricate voltammetric DA sensors. The linear range and LOD were 1–100 μM and 0.86 μM for DA. The application of the 40-fold diluted human serum samples showed satisfactory results [75]. Similarly, MWCNT-PANI NCs were electropolymerized onto the GCE to detect 5-HT in synthetic urine samples. In the presence of compounds with similar molecular structures, such as DA, UA, AA, and EP, the sensor demonstrated selective 5-HT detection. The increased current response to 5-HT at the MWCNT-PANI/GCE was correlated with the sufficient diffusion of 5-HT in the NC and the existence of π - π interactions between them [76].

Polypyrrole (PPy) offers high electrical conductivity and excellent redox properties. Pearis et al. immobilized CNTs in overoxidized PPy to detect DA in the rat brain after short-pulse stimulations. The incorporation of CNTs increased the flexibility and number of active sites as they effectively increased the intra- and interchain charge mobility along the polymer chain [77]. Similarly, the π - π^* stacking interactions among electrochemically reduced GO, MWCNTs, and PPy were utilized to construct a DA sensor that displayed a LOD of 2.3 nM. The amperometric sensor operates at pH 7.0 for DA estimation without involving any acidic solution, which could degrade DA [78]. In another report, poly (bromocresol green), magnetic NPs, and MWCNT were used for the sensitive detection of 5-HT. Platinum NP/over-oxidized PPy/rGO NCs were electrochemically synthesized onto the GCE to detect both DA and 5-HT. The linear response ranges from 0.1–250.0 μM for DA and 0.5–10.0 μM for 5-HT were recorded. The LODs for DA and 5-HT were 42 and 106 nM. The voltammetric sensor also demonstrated good selectivity amidst Na^+ , K^+ , Mg^{2+} , Ba^{2+} , Ca^{2+} , Zn^{2+} , Cu^{2+} , Fe^{3+} , Cl^- , SO_4^{2-} , AA, UA, L-cysteine, lysine, glucose, and paracetamol.

The increase in the currents (3.5 times higher) is attributed to the unique electronic structure of rGO, and the superior electron transfer properties are due to the multipore structure and high conductivity of PPy [79].

Poly(bromocresol green), Fe₃O₄, and MWCNTs were electropolymerized on the GCE for 5-HT detection. The sensor exhibited a linear range between 0.5 and 100 μM with a LOD of 80 nM. The sensor demonstrated good selectivity to 5-HT in the presence of 400-fold excess AA, 20-fold DA, 10-fold UA, 200-fold tryptophan, 150-fold L-cysteine, and 150-fold GLU, respectively. The peak current increase is due to the synergism of Fe₃O₄, MWCNTs, and poly(bromocresol green). The utilized polymer possesses high-electron-density hydroxyl groups, which leads to effective conjugation of the target to the sensor [80]. The same group fabricated a voltammetric sensor based on poly(p-aminobenzene sulfonic acid), MWCNTs, and chitosan for 5-HT detection in human serum samples. The peak current increase is attributed to the presence of MWCNTs and the conducting polymer poly(p-aminobenzene sulfonic acid) [81]. In another study, a polythionine/AuNP-based voltammetric sensor was fabricated to detect EP in serum. The enhanced EP oxidation peak was attributed to the synergistic properties of both polythionine and AuNPs [82].

A porphyrin-cored polymer film with four pentafluorophenyl rings acting as peripheral groups was used to develop a DA sensor. The electron-withdrawing fluorine atoms enabled increased electron mobility and amplification of the electrochemical signal. The linear range was 0.05–300 μM and the LOD was 0.023 μM for DA. DA in lake water and urine samples was measurable applying this sensor [83]. Block copolymer dispersed wrinkled rGO/SPCE was utilized for the simultaneous detection of AA and DA in ex vivo brain tissues from a PD mouse. In comparison with the bare SPCE, the wrinkled rGO modified ones showed better sensitivity, low LOD, and peak-to-peak separation for DA and AA in mixed solutions. The improved electrocatalytic activity of the rGO is attributed to the use of a suitable polymer dispersant [84]. Likewise, DA secreted by PC12 cells was electrochemically detected using a polymer film based on poly-celestine blue. A poly-celestine blue film of approximately 5 nm was prepared by controlled electro-polymerization onto the GCE surface. The sensor had a LOD of 1.2 nM and a sensitivity of 17.0134 μA μM⁻¹ cm⁻² for DA. In addition, DA detection in live PC12 cells after nicotine stimulation helped to study DA release dynamics in vitro [74]. Polymerization of ferulic acid on the MWCNT/GCE was performed and applied to estimate individual NADH, EP, and DA levels. The obtained linear ranges for EP and DA were 73–1406 μM and 5–120 μM. The LOD of EP and DA were 22.2 and 2.2 μM. The sensor application to pharmaceutical formulations showed good recoveries for DA and EP (Figure 5) [85]. Another study used PEDOT-rGO-Ag hybrid NC-modified sensors for the selective 5-HT detection amidst AA, UA, and tyrosine. The electrochemically active area of the NC-modified sensor was higher than that of the bare GCE, which was the active site for the oxidation of 5-HT. The LOD of 5-HT was 0.1 nM, which could be highly suitable for 5-HT detection in various sample matrices [86]. A voltammetric sensor based on poly(1,5-diaminonaphthalene) electropolymerized film was fabricated for NE detection. The sensor exhibited a linear range from 9.90 to 90.9 μM with a LOD of 1.82 μM. The sensor also demonstrated selective NE detection with no interference from AA. The sensor performance is attributed to the presence of a conductive polymer. Sensor measurements for NE in drugs were validated using a spectrophotometric method to demonstrate the reliability of the sensor [87].

To date, it has become imperative to utilize polymers as artificial electron mediators or anti-interference layers in order to prevent undesirable interference from endogenous electroactive species [88]. In several sensors, Nafion has been widely used as an anti-interference layer. The membrane can readily attract cations, eliminating anionic species such as AA and UA [89].

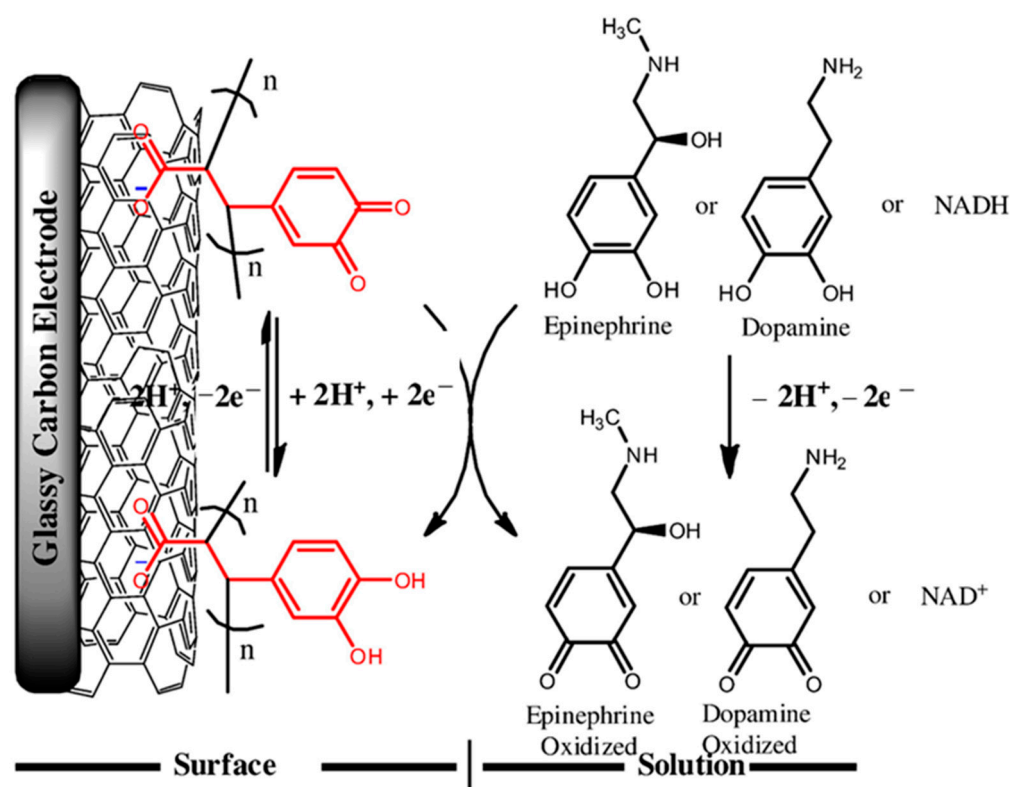


Figure 5. Schematic of the electrochemical sensor (poly-FA/MWCNTs/GCE) showing electro-oxidations of EP and DA. Reprinted with permission from ref. [85]. Copyright 2017, Elsevier.

3.3. Molecularly Imprinted Polymers (MIPs)

Generally, the preparation and electrodeposition of polymers are simple and cost-effective. Imprinting the polymer matrix with a template molecule allows for target detection. The MIPs serve as artificial receptors as they enable new insights for creating receptors by forming cavities for analyte binding in the polymer structure. The size of the formed cavities is crucial for specific chemical recognition between MIPs and NTs. The three types of chemical recognition methods are non-covalent, semi-covalent, and covalent [90]. The imprinting process is also simple because it involves a one-step polymerization method, which recommends only changing the template molecule in the polymerization solution to target various analytes of interest [91]. Thus, the electro-copolymerization of *o*-phenylenediamine and resorcinol in the presence of the template DA molecule has been applied to fabricate a DA sensor. The MIP sensor exhibited higher current response than the non-imprinted sensors, with a LOD of 0.13 μM . For application to pharmaceutical and blood samples, the MIP sensor demonstrated selective DA detection [92]. Polymerized thioaniline was imprinted using DA template. After template extraction, the imprinted polymer exhibited fast and direct detection of DA. The designed MIP sensor demonstrated a LOD of 0.033 nM [93]. A DA-imprinted polymer film of 5-amino 8-hydroxy quinoline was electrodeposited on a rGO-modified GCE, which demonstrated good affinity toward DA [41].

Graphite-paste electrodes modified with $\text{Fe}_3\text{O}_4/\text{Au}/\text{SiO}_2$ -MIP NCs were used to fabricate a voltammetric sensor for 5-HT. The sensor exhibited high sensitivity toward 5-HT, which is attributable to the synergistic effects of Fe_3O_4 and Au. After template 5-HT removal, more specific cavities were created, enhancing analyte capacity and sensitivity. The sensor demonstrated linearity from 0.01 to 1000 μM with a LOD of 0.002 μM . The sensor is highly selective to 5-HT in the presence of 100-fold increased concentrations of AA, UA, NE, and 250-fold increased concentrations of DA, GLU, ions, etc. Also, the sensor demonstrated satisfactory recoveries in pharmaceutical and urine samples, and the authors suggest that the sensor is highly suitable for point-of-care applications (Figure 6) [94].

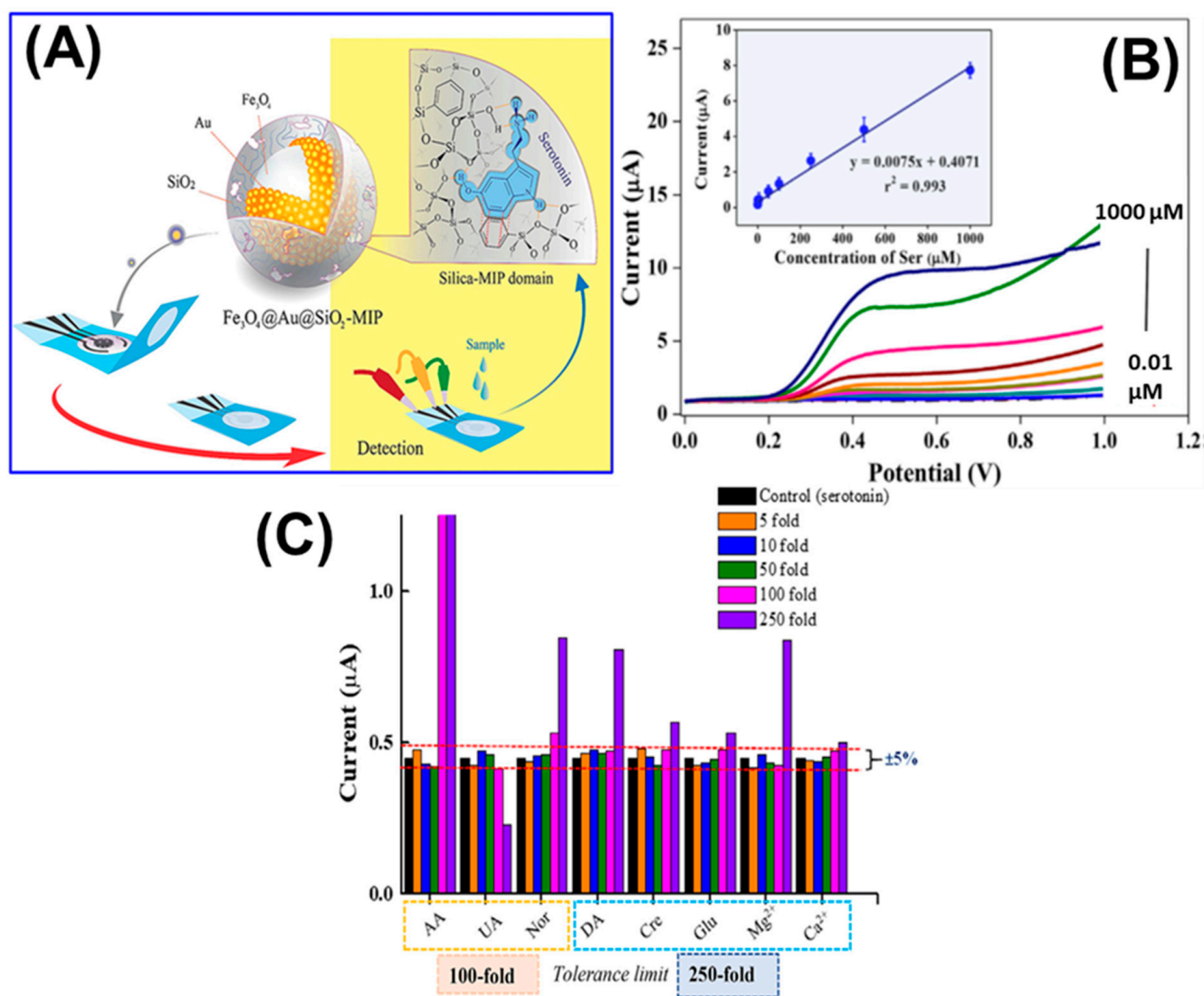


Figure 6. (A) Schematic of the paper-based MIP electrochemical sensor for 5-HT estimation. (B) Typical LSV responses of the sensor against 5-HT concentrations. Inset: calibration curve obtained for 5-HT. (C) Selectivity for 5-HT in the presence of other interfering species. Reprinted with permission from ref. [94]. Copyright 2019, Elsevier.

Until now, few studies have explored the recognition mechanism of MIPs and NTs. Research on the exact mechanisms behind target recognition should be emphasized as it could help in designing MIPs-based electrochemical sensors with even higher selectivity, sensitivity, and accuracy for clinical use. Also, the optimization of production methods, overcoming the drawbacks of electro polymerization, is a significant challenge [92–94].

3.4. Metal-Organic Frameworks (MOFs)

MOFs are porous coordinated polymers constructed using organic ligands that connect metal ions or clusters through strong coordination bonds. MOFs are an interesting option for electrochemical sensors because they offer the advantages of both organic and inorganic components. The use of MOFs in sensing applications has expanded significantly because of their exceptionally high surface area, structural flexibility, and property tunability [95]. The ordered pores and large specific surface area not only improve the loading percentage of functionalities for sensing but also offers good selectivity for specific analytes through size exclusion effects. Additionally, MOFs have a variety of architectures that can be customized by altering the functional linkers, which enables the unique functionalities of MOFs. The

analytical parameters, including the sensitivity, selectivity, reproducibility, and detection limit, can be improved by applying MOFs. Based on their exclusion size discrimination capacity, the functional groups in MOFs can significantly exclude interferences from larger molecules. The selectivity can arise from the interaction of the analyte with the linker or the structural metal [96].

Xu et al. synthesized molybdenum oxide-based MOFs coated with a conductive polymer, PPy, to detect nanomolar levels of DA via DPV [97]. Moghzi et al. have detected DA in human serum samples using a 2D MOF of a fluorescent metal-organic nanosheet of europium [98]. Similarly, Chen et al. developed porphyrin- and PEDOT-based MOF for DA detection sensitivity [99]. Yu et al. fabricated an rGO-zeolitic imidazolate framework-8 hybrid NC for sensitive DA detection. The sensor exhibited high sensitivity for DA owing to the synergism of rGO and the zeolitic imidazolate framework 8. The sensor was then applied to measure DA in human serum, which demonstrated satisfactory recoveries [100]. A water-stable conductive MOF based on Ni, Cu, and hexahydroxytriphenylene was synthesized for the voltammetric sensing of both DA and 5-HT. LOD of 63 ± 11 nM for DA and 40 ± 17 nM for 5-HT, with a linear range from 40 nM to 200 μ M, were achieved in the presence of AA and UA. Systematic investigations of these four analytes were conducted in detail, and simulated urine samples were utilized to test the practical applicability of the MOF-based sensor (Figure 7) [101]. Similarly, Xu et al. synthesized Ni-based MOFs to detect significantly lower concentrations of GLU. This ultra-low LOD is attributed to its excellent charge-transfer ability and electroactivity toward the oxidation of GLU [102].

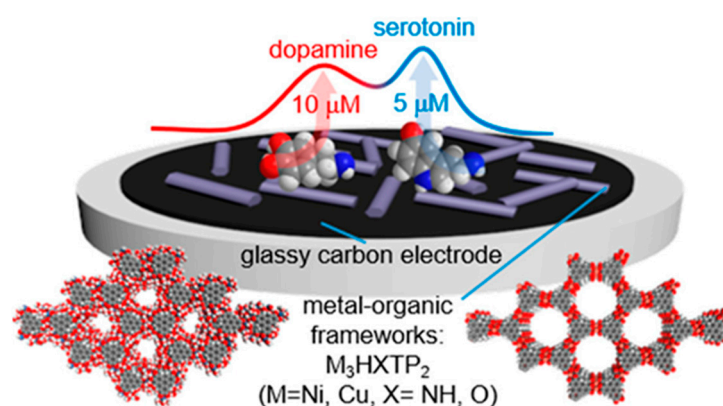


Figure 7. Schematic of the MOF-based voltammetric sensor for DA and 5-HT estimation. Reprinted with permission from ref. [101]. Copyright 2020, American Chemical Society.

Sometimes, the lack of selectivity is the strongest issue that the scientific community working on the development of new MOFs has to overcome. On designing new MOFs for sensor development, an important challenge is to highlight the control of the size, shape, and morphology in a reproducible manner. Hence, there is a persisting demand for other types of sensing materials [96].

3.5. Metals and Metal Oxide NCs

Electrochemical sensors are fabricated mainly using pure metals (Au, Pd, Ni, Pt, and Cu) and oxides (ZnO, Co₃O₄, CuO, TiO₂, and NiO). The sensing mechanism of metals is mainly due to the surface reactions involving pre-adsorbed oxygen species. Consequently, in the case of hybrid nanocomposites (metal/metal oxides or metal oxide/metal oxides) the guest metal/metal oxides serve as catalyst [17]. Because of their higher conductivity, large specific surface area, and improved catalytic characteristics, AuNPs are used as electrocatalytic material in sensors. The electron transfer properties are significantly enhanced by AuNPs, thus enhancing their sensing performances [103]. AuNPs and (polypropylene imine) dendrimers were electrodeposited onto the GCE to fabricate a sensor capable of detecting DA in serum amongst AA and EP. The NCs showed an improved electroactive

surface area and better electrochemical response to DA than bare GCE. A UV-visible spectroscopic method was employed to validate the sensor measurements, and the recovery percentages were less than or equal to 100%. Although this sensor could detect DA from 0.16 μM , the percent recovery is not 100%. However, it is challenging to detect DA in complex matrices (human serum) [104]. AuNPs and poly(hydroquinone) films were modified on nickel foam to prepare a sensitive DA sensor. The selectivity of the sensor was tested in the presence of 100 folds of glucose, UA, AA, and hydroquinone. The sensor, when applied for DA detection in two kinds of DA injections, showed good recoveries from 94.0% to 101.0%, indicating effective DA determination [105].

Similarly, PPy-decorated AuNPs were used for 5-HT detection in serum samples. The analytical performance of the sensor was 320 times greater than the bare electrode, which emphasizes the advantages of this tailored NC, PPy/AuNPs [106]. Molecularly imprinted silica (MIS)-coated PtNPs were modified on the GCE to obtain a 5-HT sensor. The sensor showed a linear response from 0.05–80 μM and a LOD of 0.02 μM . MIS composites promote selectivity and fast association/dissociation kinetics. Moreover, they can solve the issues of low binding capacity and poor site accessibility. PtNPs have large specific surface areas and high electrical conductivities. MIS-coated PtNPs exhibit the advantages of good selectivity, high sensitivity, and rapid response to 5-HT [107].

AuNPs were deposited on indium tin oxide to detect NE in blood and urine samples using square wave voltammetry (SWV) and cyclic voltammetry (CV). The linear range was 100–25 μM for NE. The LOD was 87 nM. In addition, the effect of pH revealed that the NE oxidation at the electrode involved transferring an equal number of protons and electrons. A validation study of the sensor using the HPLC method was performed to prove that the sensor was highly sensitive to NE detection [108]. MWCNT/Ti-doped ZnO NCs were prepared to fabricate a voltammetric sensor for GLU and AA. The reduction reaction of GLU was close to -0.5 V , whereas the oxidation reaction of AA was approximately 0.5 V. After Ti doping, the band gap energy of ZnO narrowed, enabling increased electron mobility. MWCNTs minimize surface fouling, resulting in better connectivity between the NC layer and the sensor. Thus, GLU detection is possible without enzyme integration [109]. AuNPs were self-assembled on the GCE using a cysteamine linker to fabricate a voltammetric EP sensor. The sensor tested with pharmaceutical samples demonstrated no interference from AA [110].

Ferrocene-AuNP/MWCNT-based NCs were modified onto the SPCE to detect 5-HT (LOD: 17 nM) using SWV in urine samples [111]. A composite based on nickel phthalocyanine, ZnO NPs, and CNT was modified on a graphite electrode to detect DA in DA-enriched human serum samples (Figures 8 and 9) [112]. MWCNTs and AuNPs immobilized carbon electrodes were used for DA and 5-HT detection in human serum, tears, and saliva samples [113]. Single and/or simultaneous DA and EP detection was done using a GCE/nickel oxide (NiO) NPs/CNTs loaded di-hexadecyl phosphate film, under SWV and DPV techniques. The developed sensor was then applied to human cerebrospinal fluid, human serum, and lung fluids to estimate the dual targets [114].

A NiO-based electrochemical sensor was fabricated for the amperometric detection of EP, NE, and DA NTs. NiO flower-like structures with head and arm-like morphology were designed to accommodate high amounts of released NTs. The enhanced catalytic activity of the sensor can be attributed to the wide surface area and multidiffusive pores in the NiO structure. A fixed applied potential of about 0.12, 0.17, and 0.21 V was revealed for NE, EP, and DA with nanomolar LODs. The proposed sensor was also applied to detect DA released from PC12 cells treated by K^+ and demonstrated good results (Figures 10–12) [115]. Likewise, a NiO/CNT/PEDOT NC was electrochemically modified on a GCE to detect three targets, DA, 5-HT, and tryptophan (Trp) in serum. The DPV results displayed three separate oxidation peaks in mixed solutions of DA, 5-HT, and Trp due to the synergism of NiO, CNT, and PEDOT. The LOD for DA, 5-HT, and Trp were 0.026, 0.063, and 0.210 μM , respectively. NiO accelerated the electrocatalytic oxidation of these targets, whereas CNTs significantly increased the electron transfer rate. PEDOT, a conductive polymer, has demonstrated an

affinity for the target. These combined properties enable the simultaneous detection of these three analytes [116].

Flower-shaped ZnONPs/PANI/rGO was electrodeposited onto the GCE to estimate DA in human and drug samples. The LOD was 0.8 nM for DA. The sensor showed high electroactivity toward DA because of the improved surface area and conductivity of ZnO nanoparticles. Additionally, using a conducting polymer with a porous rGO structure enhances the electrocatalytic properties of ZnONPs [117]. Similarly, MWCNT–ZnO/chitosan (CS) NC-modified SPCE was used to simultaneously detect NE and 5-HT using SWV. The high catalytic activity of the NCs enhanced the current responses to the targets. NE and 5-HT peak potentials were at approximately 90 and 280 mV, respectively. A LOD of 0.2 μM and 0.01 μM was attained for NE and 5-HT. When applied to rat cerebrospinal fluid samples, the sensor demonstrated good selectivity and sensitivity to both targets. MWCNTs and ZnONPs were responsible for the electron transport and electrochemical activity of the sensor. CS has significant properties, such as membrane-forming ability, ion exchange and transport. The combined advantages of MWCNTs, ZnONPs, and CS NCs ensure that the simultaneous determination of these two targets is highly feasible [118].

Fe_3O_4 , ZnONP-doped phthalocyanine, and functionalized MWCNTs were used to fabricate a voltammetric EP sensor. EP and NE electro-oxidation on the MWCNT/ Fe_3O_4 -ZnONPs-Pc/GCE was mainly diffusion-controlled, with negligible adsorption of reaction products. The sensors detected EP and NE amongst AA and were found to be stable, reusable, and resistant to fouling effects after long scans [119]. An amperometric array sensor based on Pt-coated Ni nanowires was developed to detect GLU. The array sensor sensitivity was found as 96 $\mu\text{A mM}^{-1} \text{cm}^{-2}$ with a LOD of 83 μM . Although the sensor demonstrated good sensitivity, its detection limit was still higher and not sufficient to meet real-time measurement challenges [120].

Metal molybdates offer richer redox active sites than single-component oxides because of their combination of iron and molybdenum ions. An iron (II) molybdate (FeMoO_4) nanorod-modified GCE was used to fabricate a voltammetric NE sensor. The sensor demonstrated good sensitivity with the lowest LOD of 3.7 nM. The FeMoO_4 nanorods showed maximum current responses toward NE, which is attributed to the polycrystalline nature of the nanorods, which enhanced electron transport [121].

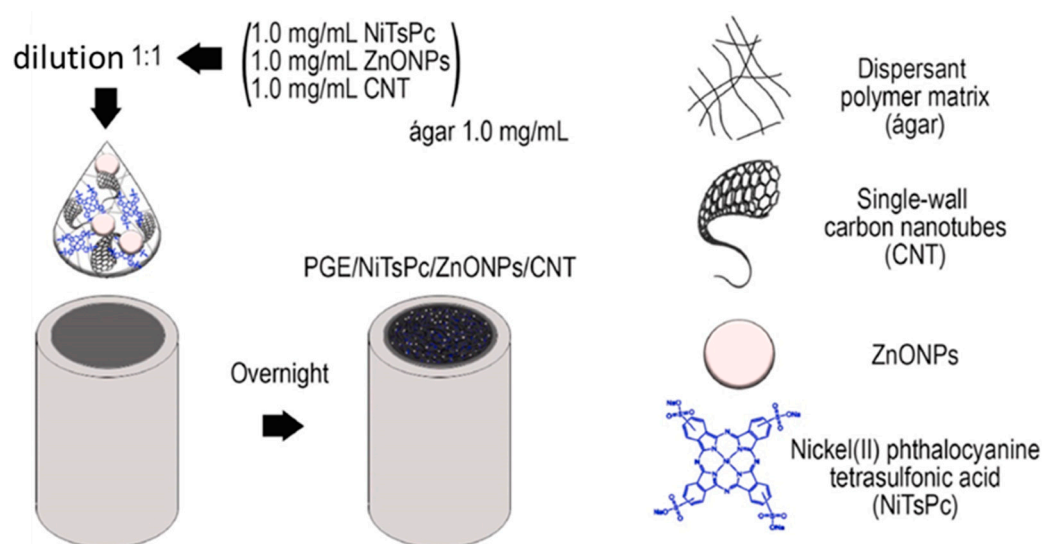


Figure 8. Schematic of the voltammetric sensor for DA detection. Reprinted with permission from ref. [112]. Copyright 2022, Elsevier.

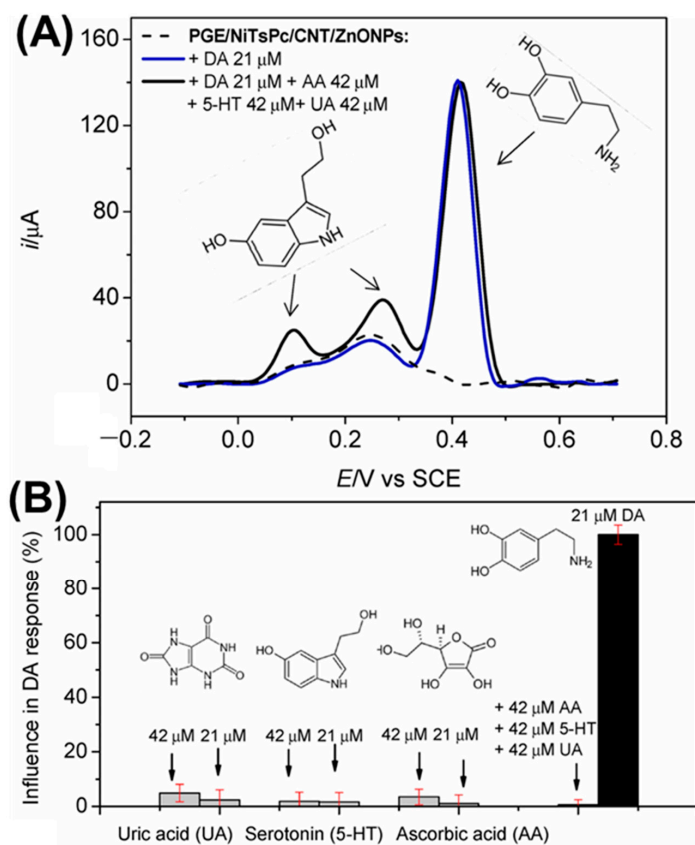


Figure 9. (A) DPVs recorded for DA in the presence of other biomolecules. (B) Compares the DA signals with UA, 5-HT, and AA signals using DPV. Reprinted with permission from ref. [112]. Copyright 2022, Elsevier.

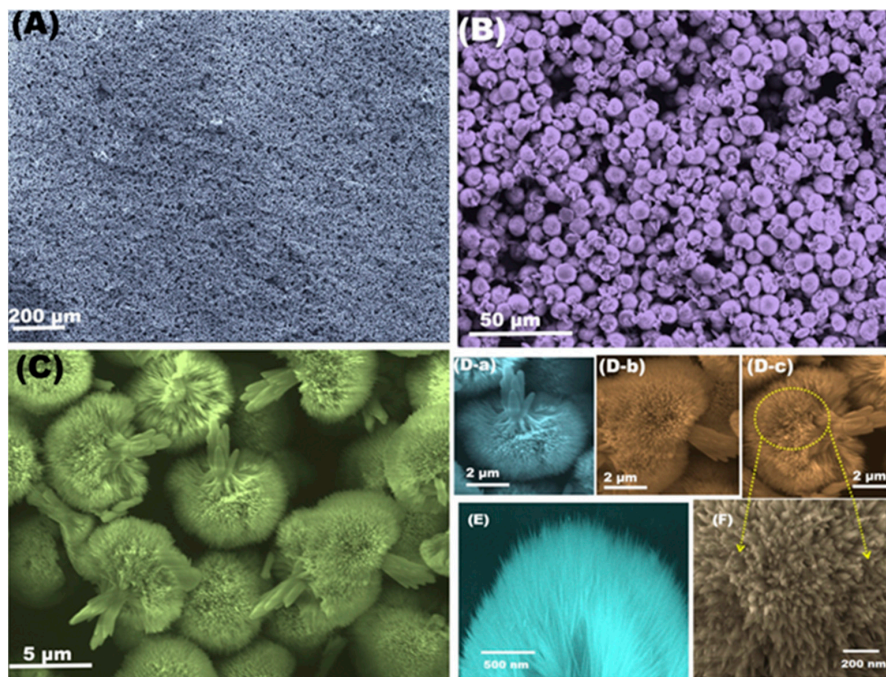


Figure 10. (A,B) Scanning electron micrographs of NiO/ITO. (C) High magnification FE-SEM of NLF, which shows the flower-like structures of NiO. (D-a–D-c) FE-SEM at different positions. (E,F) high magnification of small sections that reflect the needle-like morphology. Reprinted with permission from ref. [115]. Copyright 2018, Elsevier.

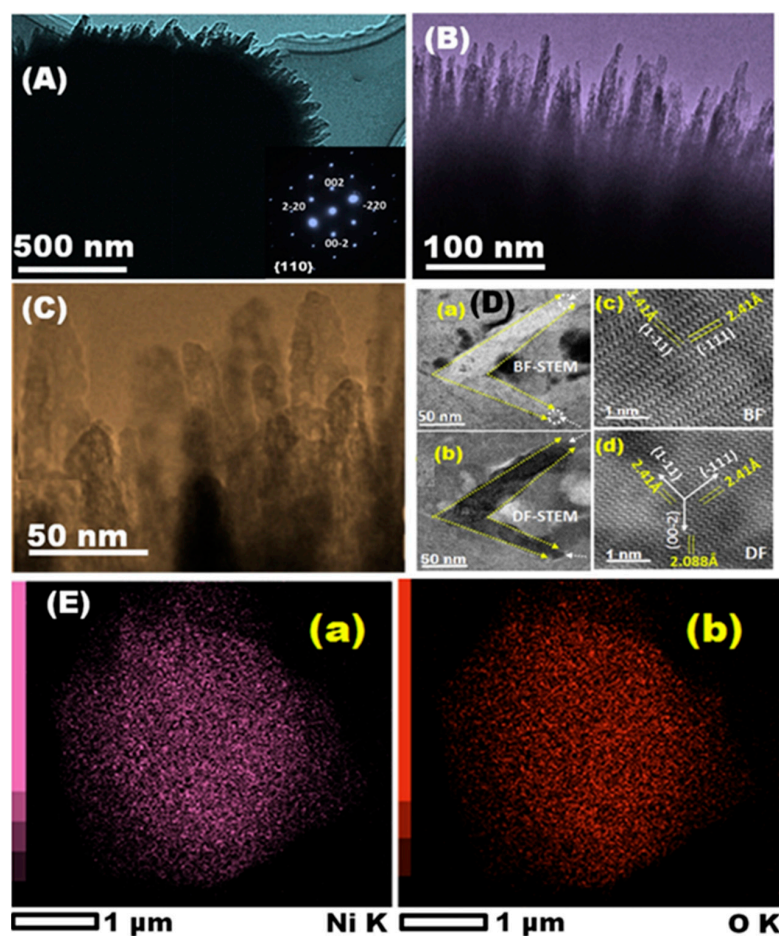


Figure 11. (A,B) Scanning transmission electron micrograph showing cross-section of the NiO. (C,D) the head needle ends illustrating defined pores; (D-a–d) the high crystalline degree of NiO with $d\{110\} = 2.41 \text{ \AA}$ with dominant $\{110\}$ plane of inter-faces. (a,b) scale bar: 50 nm (c,d) scale bar: 1 nm indicating the porous surfaces of the needle ends. inset of (A) NiO electron diffraction pattern. (E-a,b) NiO EDS mapping. Reprinted with permission from ref. [115]. Copyright 2018, Elsevier.

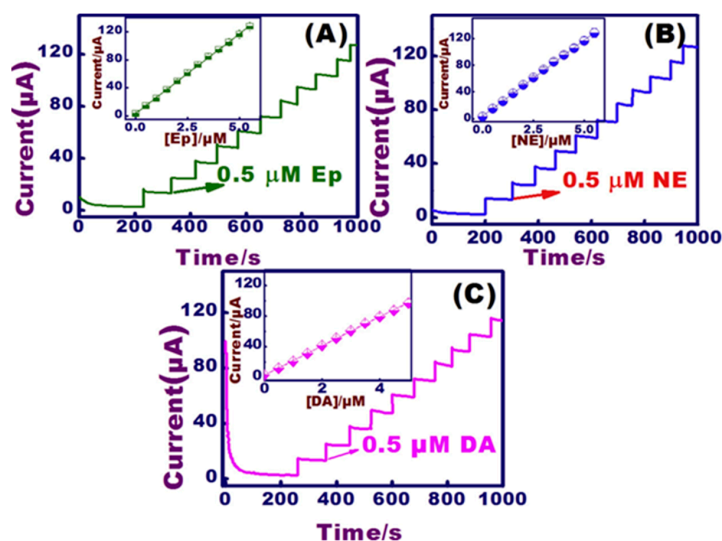


Figure 12. CA responses of (A) EP, (B) NE, and (C) with successive DA additions (0.5 to 5 μM), inset the DA linear plot on NiO modified sensors at the constant applied potentials (0.12, 0.17, and 0.21 V for EP, NE, and DA). Reprinted with permission from ref. [115]. Copyright 2018, Elsevier.

3.6. Transition Metal Oxide, Carbide, and Sulfide NCs

Over the past two decades, transition-metal oxides have attracted much interest in sensing applications owing to their superior electronic and magnetic properties, catalytic activity, and ease of preparation and modification processes. Transition metal oxides act as peroxidase mimics and have been integrated into the sensor fabrication processes. Mixed metal oxide CuO-MgO NC-based sensors were synthesized to detect DA in artificial sweat. The sensor exhibited a linearity from 10–100 μM , a high sensitivity of $69 \mu\text{A mM}^{-1} \text{cm}^{-2}$ and a LOD of 6.4 μM . CuO-MgO NC exhibits a high surface area, and enhanced conductivity, which aids in fast electron transfer to and from DA [122]. Fe_3O_4 , ZrO_2 , and GO NC were used to fabricate DA sensors. The sensor sensitivity was $3.649 \mu\text{A } \mu\text{M}^{-1} \text{cm}^{-2}$, and the LOD was 0.1562 μM , with a linear range of 0.5–15 μM . The enhanced sensitivity and LOD of the sensor were attributed to the possible synergistic amplification of Fe_3O_4 , ZrO_2 , and GO [123]. Kokulnathan et al. prepared an amperometric sensor based on Fe_2O_3 NP-capped graphene sheets to monitor trace levels of DA (LOD:0.001 μM) in human serum and urine samples [124]. Vinay et al. modified a CPE with Fe_2O_3 to construct a voltammetric sensor that could measure DA in drug and serum samples [125].

MnO_2 -graphene composite was used to fabricate a voltammetric sensor for 5-HT. The coupling of MnO_2 with graphene enhanced the specific surface area, which improved electron transport, opening numerous channels for the target diffusion. Quantification of 5-HT by SWV exhibited linear range of 0.1 to 800 μM with a LOD of 10 nM. The sensor also exhibited high reproducibility and anti-interference ability [126]. Fe_2O_3 NPs were combined with two redox polymers, poly (brilliant cresyl blue) and poly(Nile blue), to fabricate a sensor capable of measuring EP in adrenaline injections in the presence of ascorbic acid [127]. Ardakani et al. electrodeposited Fe_2O_3 NPs onto a GCE for levodopa detection, DA, and EP, with LOD of 24, 14, and 12 nM, respectively [128].

MXenes exhibit good electrical conductivities and negatively charged surfaces for DA detection. Shahzad et al. developed a DA sensor using Nafion-stabilized two-dimensional transition metal carbides ($\text{Ti}_3\text{C}_2\text{Tx}$ MXenes). $\text{Ti}_3\text{C}_2\text{Tx}$ was drop-coated on the GCE, followed by Nafion coating, to obtain a sensitivity of approximately 3 nM [129]. Meijun et al. constructed a DA sensor based on Ti_3C_2 MXenes, graphitized MWCNTs, and ZnO nanospheres. A much lower LOD of approximately 3.2 nM was achieved in human serum samples [130]. TiO_2 /MXene with a polyvinyl alcohol/GO NC-based hydrogel was formulated to detect NE in the urine samples. The efficient electrocatalytic activity of TiO_2 , high conductivity of MXene, and sample loading via the PVA/GO hydrogel promoted NE electro-oxidation. The sensor results for urinary samples were validated by HPLC, which demonstrated sensor sensitivity for NE detection [131]. Molybdenum trioxide (MoO_3) nanowires were used for NE detection via CV and CA experiments. The sensor exhibited the lowest LOD of 0.11 μM . The electrochemical performance is due to the high catalytic activity of the MoO_3 nanowires, which provides a path for electron transport, thereby increasing sensor sensitivity [132].

Molybdenum disulfide (MoS_2), a transition metal sulfide, consists of three atomic layers (S–Mo–S) stacked together by van der Waals forces [133]. A simple sensor based on the one-step electrochemical deposition of NCs consisting of MoS_2 , MWCNTs, and PPy to estimate DA levels in the brain tissue of a PD mouse was reported. The sensor exhibited a sensitivity of $1.130 \mu\text{A } \mu\text{M}^{-1} \text{cm}^{-2}$, a dynamic linear range of 25–1000 nM, and a LOD of 10 nM for DA [134]. Borocarbonitrides are structural analogs of graphene. The MoS_2 -rGO composite and borocarbonitride were used as electrode modifiers to selectively detect DA and UA amidst AA. The composite demonstrated high electrocatalytic activity owing to its enhanced electronic conductivity, large surface area, and available edges, which facilitated sufficient electron transfer [135]. Tin disulfide (SnS_2)-decorated graphene- β -cyclodextrin NCs were developed for DA detection. The SnS_2 /graphene- β -cyclodextrin sensor showed selective DA detection in the presence of 50-fold addition of common interfering species. The fabricated sensor demonstrated a sensitivity of $2.49 \mu\text{A } \mu\text{M}^{-1} \text{cm}^{-2}$ with a LOD of 4 nM for DA. The sensor was then utilized for DA detection in rat brains and human blood

serum samples. The recovery of DA in rat brain samples suggests that this NC could be used for the design of electrochemical sensors (Figures 13 and 14) [136].

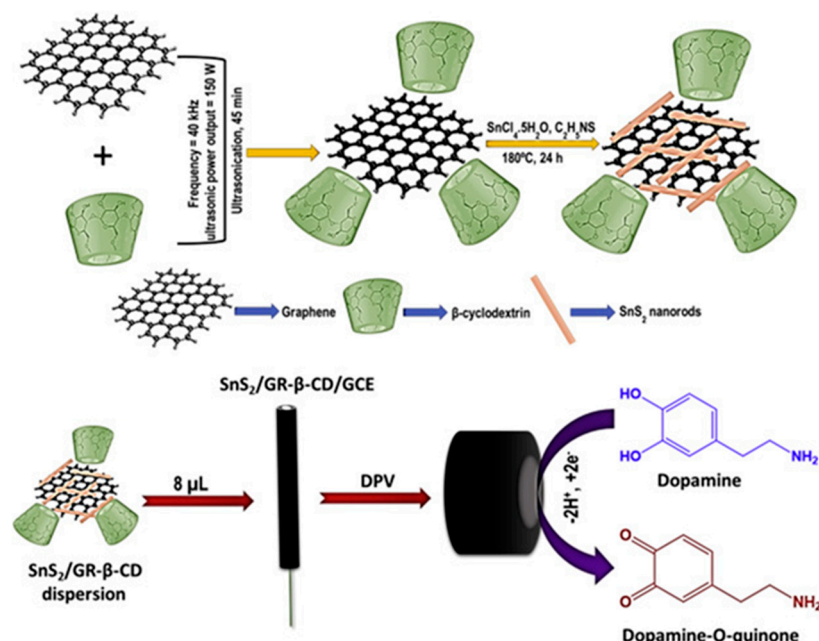


Figure 13. Schematic of SnS₂/graphene-β-CD NC modified sensors for DA sensing. Reprinted with permission from ref. [136]. Copyright 2019, Elsevier.

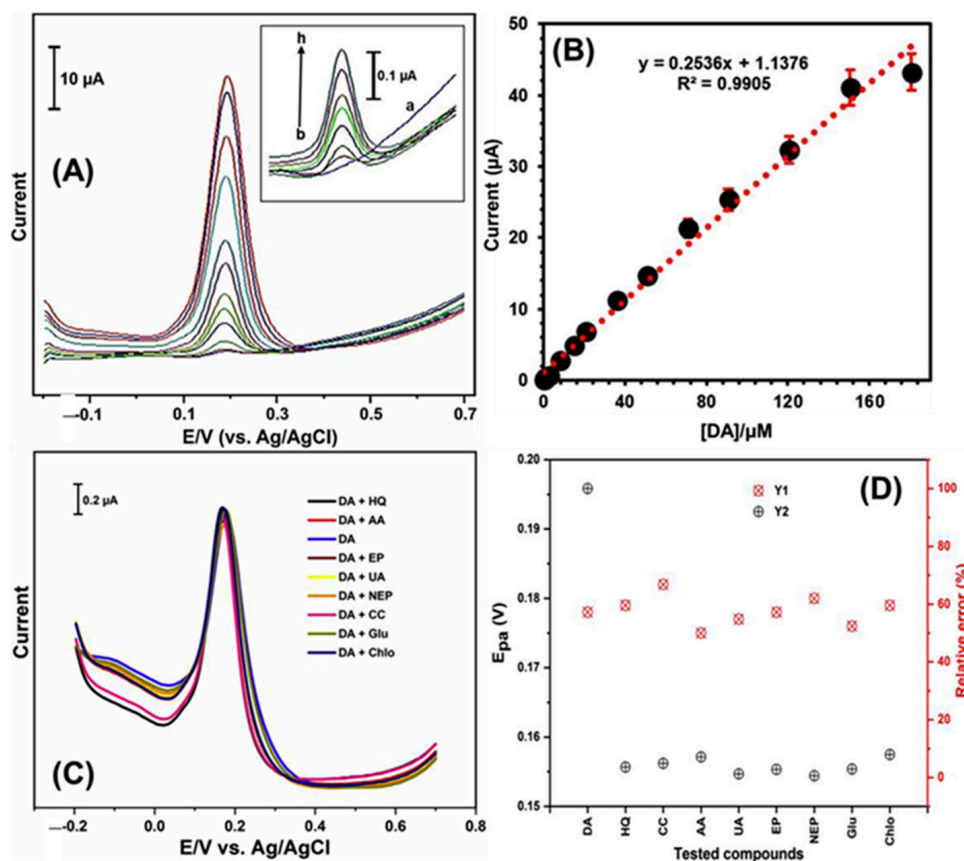


Figure 14. (A) DPV results of SnS₂/graphene-β-CD NC modified sensors against different concentrations of DA. Inset of (A) shows the DPV response of the sensor in the (a) absence and (b-h) presence of different

concentrations of DA. **(B)** Calibration plot. **(C)** DPV responses of the sensor against 0.5 μM DA and 25 μM addition of possible interferences such as hydroquinone, catechol, AA, UA, EP, and NE. **(D)** The oxidation potential of DA (Y1) and its relative error (Y2). Reprinted with permission from ref. [136]. Copyright 2019, Elsevier.

3.7. Ionic Liquids

Room-temperature ionic liquids (IL) possess good solvating properties, high conductivity, low toxicity, and sufficient electrochemical stability. They can also act as binders for CNTs. A voltammetric sensor with CNTs and IL was fabricated for the simultaneous measurement of 5-HT and DA. The linear range of the sensor was from 20 nM–7 μM for 5-HT and 0.1–12 μM for DA. LODs of 8 nM and 60 nM for 5-HT and DA were acquired [137]. A voltammetric sensor based on IL-functionalized graphene was used for the simultaneous 5-HT and DA detection in human serum samples. The ionic conductivity of the IL accelerated the electron transfer rate of the targets. In addition, the combined advantages of graphene and IL have promoted dual-target detection. The results showed that the 50-fold excess AA and UA did not interfere with the detection of 10 μM of 5-HT and DA [138].

A carboxyl-functionalized mesoporous material/colloidal Au-modified nanocarbon IL paste electrode was initiated for 5-HT estimation. The sensor showed a linear response between 0.2–20 μM and a LOD of 0.1 μM for 5-HT applying the SWV technique. The nanocarbon IL sensor has advantages such as easy fabrication, fast electron transfer, and good antifouling abilities. Colloidal Au is well-known for its excellent catalytic activity. Mesoporous materials exhibit high surface areas, controllable pore sizes, and ordered pore structures. The synergistic properties of these NCs play a crucial role in the electrochemical performance of sensors [139]. MWCNTs functionalized with benzofuran derivatives and IL were utilized to fabricate a voltammetric sensor for the dual detection of NE and 5-HT. The sensor exhibited two linear ranges for NE and one linear range for 5-HT with a LOD of 49 μM and 2 μM for NE and 5-HT. The synergism of the CNTs and IL effectively enhanced the sensor conductivity [140].

3.8. Other NCs

Copper selenide was hydrothermally synthesized and electrodeposited to detect trace levels of DA in the presence of AA and UA. The redox activity of the Cu center is believed to enhance the rate of DA oxidation on the electrode. It is claimed as the first report employing selenides to detect DA [141]. Gadolinium orthoferrite NPs and graphite paste were mixed at a ratio of 1:4 to fabricate the DA sensor. The sensor illustrated a LOD of 700 nM, with a linearity from 5 μM to 160 μM for DA [142].

Bismuth sulfide (Bi_2S_3) has evoked enormous interest in the field of electrochemistry because of the presence of free electrons rather than holes, thus serving as a major electron carrier. Yan et al. prepared Bi_2S_3 nanorod-rGO NCs to detect urinary DA levels. The sensor exhibited a good linearity (0.01–40 μM) and a LOD of 12.3 nM. The enhanced sensor performance is attributed to the synergism of the rGO sheets and Bi_2S_3 nanorods, which accelerated electron transport and extended the catalytic active sites for DA sensing. In addition, the size of the NC was tunable by adjusting the GO loading [143]. Ramachandran et al. used pulverized graphite (pGr) obtained via mechanical ball milling for the fabrication of DA sensors. The sensor successfully detected DA in the biological samples. Effective DA sensing on pGr is attributed to its intact aromatic structures. The sensing performance of pGr toward DA and AA is argued to be superior to those of rGO and GO [144].

Graphene-encapsulated AuAg nanohybrids were employed as electrocatalysts for sensitive 5-HT evaluation in human serum. The sensor displayed a wide linear range (2.7 nM to 4.82 μM), and a very low LOD (1.6 nM) with only negligible interferences. This is due to the enhanced catalytic activity of the graphene-encapsulated AuAg nanohybrids, which possess monodispersed AuAg catalysts with greater electrochemical active sites [145]. An electrochemical microfluidic paper-based sensor based on graphite-chitosan-polyethylene glycol electrodes modified with graphene and sodium dodecyl sulfate surfactant was for-

mulated to measure DA in blood and urine samples. The paper-based sensor exhibited good sensitivity, as well as short detection time [146].

Siloxene is a semiconductor with a 2D structure, usually prepared through the deintercalation of calcium from calcium silicide (CaSi₂). Unlike the planar graphene structure, siloxene has a low-buckled honeycomb lattice structure with mixed sp² and sp³ hybridization bonds [147]. Planar Si structures with interconnected Si₆ rings and large surface areas enable the application of siloxene in sensor development [148].

To customize the electrocatalytic characteristics of metallophthalocyanine complexes, their molecular architectures can be changed. Changing the central metal or introducing substituents into the phthalocyanine rings has a powerful influence on their electrochemical sensing properties. Owing to these features, metallophthalocyanine has found wide application as a sensing material for the detection of a variety of analytes [149]. Graphene sheets with cobalt tetrasulfonated phthalocyanine were modified onto GCE to sensitively detect DA in the presence of high concentrations of AA and UA with a LOD of 0.87 nM and a linear range from 20 nM to 220 nM. The sensor had excellent selectivity for low concentrations of DA amongst high concentrations of AA and UA. The negatively charged cobalt tetrasulfonated phthalocyanine prevents the adsorption of negatively charged AA and UA on the sensor [150]. PPy-modified SPCE was also doped with green-synthesized Fe₃O₄NPs from *Callistemon viminalis* leaves and flower extracts. The modified sensors demonstrated good electrocatalytic activity toward 5-HT detection [151].

Graphite, nanodiamonds, and AuNPs were modified onto the GCE using casein biopolymer to construct a voltammetric sensor for 5-HT estimation. The sensor displayed a linear response from 0.3 to 3.0 μM, and a LOD of 0.1 μM. The sensor on testing with synthetic urine samples exhibited good recovery (91.4 to 103%). The presence of nanodiamonds and AuNPs increased the active surface area and electron transfer rate from 5-HT to the sensor. Detecting 5-HT in urine samples could enable easy diagnosis of NDs [152]. Nafion/Ni(OH)₂-MWCNTs modified GCE was used for the simultaneous DA and 5-HT detection. Due to the synergistic electrocatalytic effects of MWCNTs with Ni(OH)₂ NPs, electron transfer was feasible. The negatively charged Nafion film promoted selective DA oxidation and elimination of the interference from AA. The sensor showed a linearity of 0.05–25 μM with a LOD of 0.015 μM for DA and 0.008–10 μM with a LOD of 0.003 μM for 5-HT, respectively [153]. Table 1 compares the analytical parameters of nanocomposite-based electrochemical sensors for DA, 5-HT, GLU, EP, and NE detection.

Table 1. Comparison of the analytical parameters of nanocomposite-based electrochemical sensors for DA, 5-HT, GLU, EP, and NE neurotransmitters detection.

Target	NC Modification	Linear Range (μM)	LOD (μM)	Sensitivity (μA μM ⁻¹ cm ⁻²)	Electrochemical Technique	Tested Real Samples	Reference
DA	rGO/3D porous PU	0.0001–0.00115	0.000001	-	DPV	Human serum and urine	[37]
	rGO/Bi ₂ S ₃ /GCE	0.01–40.0	0.0123	2.046	CV, DPV	Human urine	[143]
	rGO-poly(FeTFPP)/GCE	0.05–300	0.023	-	CV, EIS, DPV	Human urine and lake water	[83]
	rGO-ZIF-8/GCE	0.10–100	0.03	0.153	CV, DPV	Human serum	[100]
	rGO-Cu ₂ O/GCE	10.0–900	0.05	0.520	CV, DPV	Human blood and urine	[154]
	Poly-FA/MWCNT/GCE	5.00–120	2.21	0.037	CV, CA	Pharmaceutical samples	[85]
	PGr/GCE	0.005–1.0	0.001	0.004	CV, DPV	Human blood	[144]
	CPE/GO	0.08–2.30	0.0086	0.489	Chrono-coulometry	Human blood	[155]
	HNP-AuAg/GCE	5.00–335	0.20	0.399	CV, DPV, CA	-	[156]
	HNP-Pt-Ti/GCE	0.004–500	3.20	0.186	CV, DPV, CA	Human serum	[157]
NiO-CuO/Graphene/GCE	0.50–20.0	0.170	9.406	CV, EIS, SWV	Human serum and pharmaceutical samples	[158]	

Table 1. Cont.

Target	NC Modification	Linear Range (μM)	LOD (μM)	Sensitivity ($\mu\text{A } \mu\text{M}^{-1} \text{cm}^{-2}$)	Electrochemical Technique	Tested Real Samples	Reference
DA	3D Macroporous carbon aerogel	0.20–90.0	-	0.030	CV, DPV, CA	Human serum	[36]
	Wrinkled rGO/SPCE	0.10–300	0.134	-	CV, LSV	Mouse brain tissues	[84]
	rGO/PAP/GCE	0.01–100	-	0.0075	CV, EIS, DPV, CA	Human serum	[39]
	Au/P-doped Graphene	0.10–180	-	0.002	CV, DPV, CA	Human serum and urine	[43]
	GQDs- MWCNTs/GCE	0.25–250	0.095	0.520	CV, EIS, DPV, CA	Human serum	[54]
	poly-celestine blue/GCE	0.01–0.7 1.0–10.0	0.0012	17.01	CV, EIS, DPV	PC12 cell lines	[74]
	MWCNT-PANI/GCE	0.0000001– 0.000012	0.000000033	-	CV, EIS, DPV	Artificial urine	[76]
	rGO/MWCNTs/PPy	0.025–0.1	0.0023	8.96	CV, EIS, CA	-	[78]
	Pt NPs/PPy/rGO	0.1–250.0	0.042	-	CV, EIS, DPV	Human blood	[79]
	MIP electrode	0.0000005– 0.00004	0.13	-	DPV	Human blood and pharmaceutical samples	[92]
	Thioaniline-AuNPs/MIP	0.000000001– 0.000005	-	0.0000038	CV, EIS, DPV	Human serum	[93]
CuTRZMoO4/PPy/GCE	1.0–100.0	0.08	-	CV, EIS	Human serum	[97]	
Porphyrin MOF/PEDOT/	4.0–100.0	-	0.011	CV, DPV	-	[99]	
5-HT	GO-g-PLA-Pd	0.10–100	0.08	-	CV, EIS, CA	-	[159]
	rGO/PANI/AuNPs-MIPs	0.20–10.0	0.0117	-	CV, DPV, Chrono-coulometry	Human blood	[160]
	rGO-Co ₃ O ₄	0.10–51.0	48.7	22	CV, EIS, DPV	Human blood	[161]
	Nafion/Co(OH) ₂ -MWCNTs	0.05–75.0	0.023	-	CV, DPV, CA	Human serum	[162]
	CNT/IL	5.00–900	2.00	-	CV, EIS, DPV, LSV	Human blood and water	[150]
	poly(bromocresol green)/GCE	0.50–100	0.08	-	CV, DPV	Human serum	[80]
	poly(p-aminobenzene sulfonic acid)/MWCNT/CS	0.10–100	0.08	-	CV, EIS, DPV	Human serum	[81]
	Fe ₃ O ₄ /Au/SiO ₂ /MIP	0.01–1000	0.002	-	LSV	Human urine and pharmaceutical samples	[94]
GLU	NiO/CS/GCE	1000–8000	272	0.011	CV, CA	-	[163]
	Co ₃ O ₄ nanosheets/GCE	0.0001– 1,000,000	0.00001	0.00095	CV	Human serum and urine	[164]
	Pt/NiNAE	500–8000	83	0.096	CV, CA	-	[120]
	NiMOF/GCE	0.005–500.0	0.00167	-	CV	Human urine	[102]
	PNIPAM/4-VP/MAA GluBP/AuNP/SPCE	- 0.10–0.8	1.7 0.15	0.0086 0.0011	CV, EIS CV, EIS	- -	[165] [166]
EP	Paraffin/MWCNT/CoPc	1.33–5.50	0.0156	5.920	CV, DPV	Human urine	[167]
	p-FA/MWCNT/GCE	73.0–1406	22.2	0.004	CV, CA	Pharmaceutical samples	[85]
	NiONPs-MWCNT-DHP/GCE	0.3–9.5	0.082	0.390	CV, DPV, SWV	Human urine, cerebrospinal and lung fluids	[114]
	EDDPT/GO/CPE	1.5–600	0.65	0.076	CV, CA, DPV	Human serum and pharmaceutical samples	[45]
	MWCNT-CS	0.05–10	0.03	-	CV, EIS, DPV	Artificial urine and pharmaceutical samples	[64]
	Graphene film	0.6–120	0.4	-	CV	Pharmaceutical samples	[168]
C-Ni/GCE	0.2–80	6.0	-	CV, DPV	-	[169]	

Table 1. Cont.

Target	NC Modification	Linear Range (μM)	LOD (μM)	Sensitivity ($\mu\text{A } \mu\text{M}^{-1} \text{cm}^{-2}$)	Electrochemical Technique	Tested Real Samples	Reference
NE	rGO–MnO ₂ /GCE	0.2–800	0.02	-	CV, SWV	Human urine	[170]
	Co ₃ O ₄ /SPCE	0.1–1525	0.075	-	CV, EIS, CA	Human serum and urine	[171]
	ATO/MIP/SWCNT/GCE	0.099–15	0.033	-	CV	Human blood	[172]
	Graphene/Pd	0.099–15	0.07	0.0174	CV, EIS, SWV	Human urine and pharmaceutical samples	[46]
	DSWCNTs/SPCE	0.1–2.0	0.062	-	CV, DPV	Rat brain	[59]
	poly(1,5-diaminonaphthalene)	9.90–90.9	1.82	-	CV, DPV	Pharmaceutical samples	[87]

PU, polyurethane; Bi₂S₃, bismuth sulfide; poly(FeTFPP), 5,10,15,20 tetrakis (pentafluorophenyl)–21H,23H-porphyrin iron (III) chloride; ZIF-8, zeolitic imidazolate; Cu₂O, copper(I) oxide; Poly-FA, polyferulic acid; PGr, pulverized graphite; CPE, carbon paste electrode; GO, graphene oxide; HNP, hierarchical nanoporous; AuAg, gold silver; PtTi, platinum titania; NiO, nickel oxide; CuO, copper oxide; PAP, p-aminophenol; g-PLA-Pd, polymerized poly(lactic acid) and palladium; PANI, polyaniline; MIPs, molecularly imprinted polymers; Cu-TRZMoO₄, molybdenum oxide-based three-dimensional MOFs with helical channels; Co₃O₄, cobalt tetroxide; Co(OH)₂, cobalt (II) hydroxide; CNT, carbon nanotubes; IL, ionic liquid, NIO, nickel oxide; CS, chitosan; Co₃O₄, cobalt oxide; Pt, platinum; NiNAE, nickel nanowire array; PNIPAM, poly-N-isopropyl acrylamide; 4-VP, 4-vinyl pyridine; MAA, methacrylic acid; GluBP, glutamate-binding protein, CoPc, cobalt phthalocyanine; poly-FA, electropolymerized ferulic acid; NiONPs, nickel oxide nanoparticles; DHP, dihexadecylphosphate film; EDDPT, 2-(5-Ethyl-2,4-dihydroxyphenyl)-5,7-dimethyl-4H-pyrido[2,3-d][1,3]thiazine-4-one; C-Ni, carbon-coated nickel magnetic nanoparticles; MnO₂, manganese dioxide; Co₃O₄, cobalt tetroxide; ATO, antimony-doped tin oxide; Pd, palladium.

4. Versatile Electrochemical Technique in NTs Analysis

Fouling typically poses a persistent challenge in the electrochemical analysis of NTs. Important NTs, such as DA, 5-HT, and NE, easily oxidize, forming an adhering insulating film on the sensor surface, which diminishes the sensor responses. Therefore, these NTs often exhibit real-time measurement problems that hamper sensor selectivity. To address this issue, electrochemical sensors modified with functional NCs were analyzed using new electrochemical techniques [173]. Fast scan cyclic voltammetry (FSCV) is a versatile tool for evaluating the fast changes in the release and uptake of NTs. In particular, DA, 5-HT, and NE can be oxidized at a specific applied potential at a rapid scan rate of 1000 V/s providing selective detection based on the applied potential-dependent oxidation and reduction processes. Based on this aspect, the functioning of DA and 5-HT in the caudate of anesthetized rat brains using the FSCV technique revealed that the uptake dynamics of 5-HT are three-fold slower than DA uptake [174]. While FSCV experiments are extended to several hours, the shape of the DA waveform and its generated color plot reveals only a plot for a few seconds to a few minutes time scale, which is considered to be significant. Through this detailed analysis procedure, waveforms for specific analytes could be customized and electrode drift could be removed using filters to visualize data on the minute-to-hour time scale [175]. The current focus of electrochemical research is on customizing waveforms for specific targets and improving their continuous monitoring [176]. The data recorded by FSCV is qualitative, as it permits the identification of the target neurotransmitter and its kinetic behavior in brain tissues with sub-second resolution. Jo et al. used carbon fiber to differentiate NE and DA signals by applying a dual electrochemical recording of FSCV and normal pulse voltammetry (Figures 15 and 16) [177].

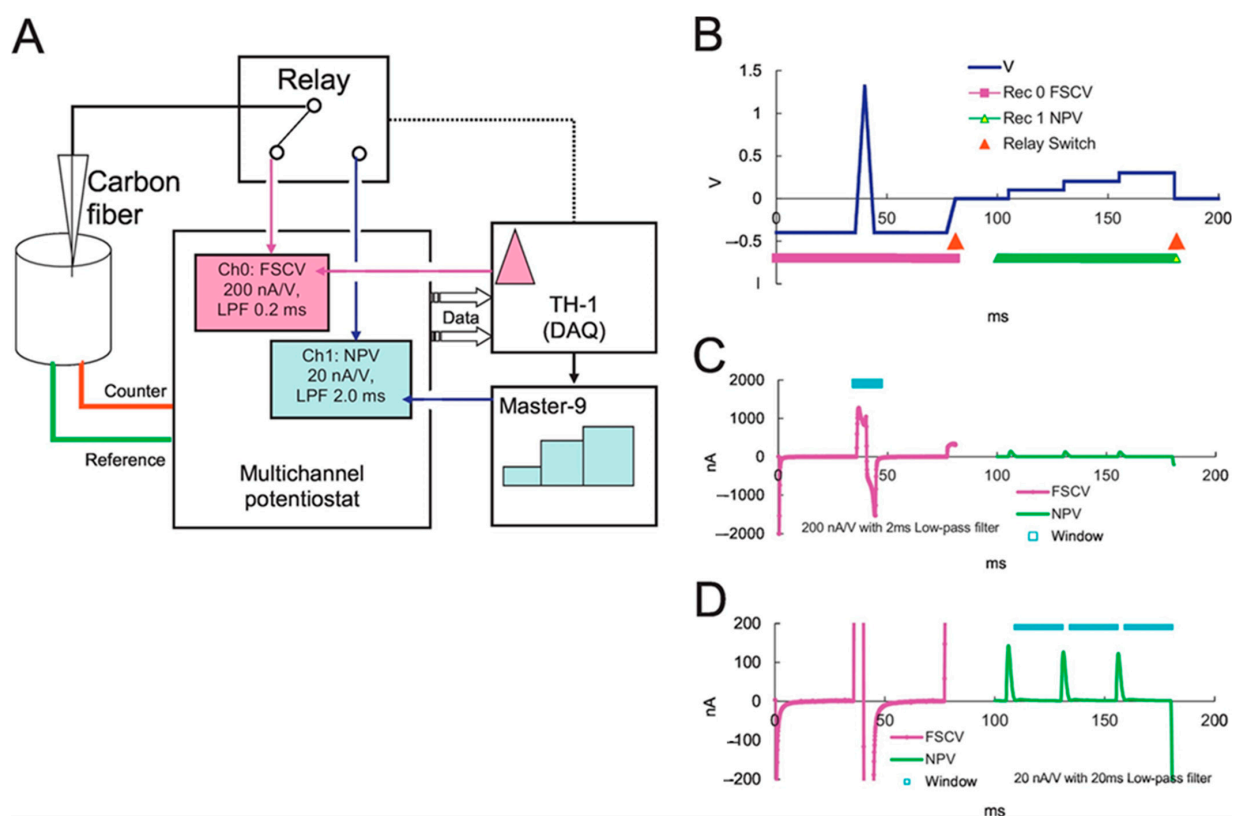


Figure 15. (A) Dual voltammetry. (B) Circuit for the dual voltammetric techniques. (C,D) Combined waveforms of FSCV and NPV. Reprinted with permission from ref. [177]. Copyright 2017, Elsevier.

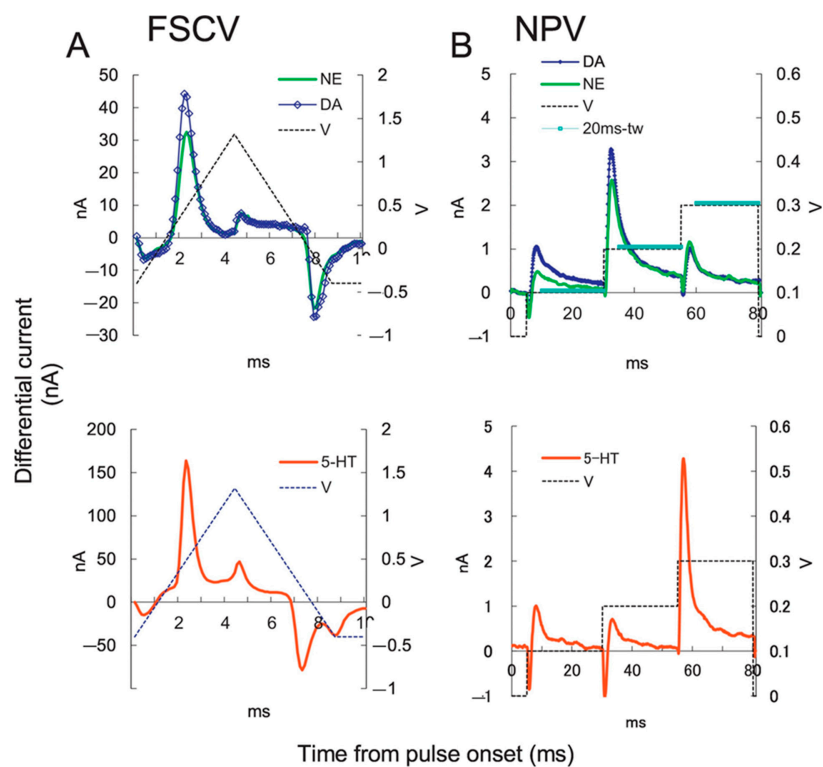


Figure 16. Current responses of NTs: (A) Current-time curve of FSCV of 1 μ M NE (green), DA (blue diamond), and 5-HT (red). The applied potential (blue dotted line), (B) NPV current-time curve. The 20 ms time windows (blue lines). Reprinted with permission from ref. [177]. Copyright 2017, Elsevier.

Fast cyclic square-wave voltammetry (FCSWV) was combined with large-amplitude cyclic square-wave voltammetry (CSWV) to differentiate DA from EP and NE. The combination of large amplitude and square-shaped potential-induced cycling through multiple redox reactions within a single square-wave pulse increases sensitivity and selectivity. Combining these two techniques, DA release in the rat striatum has been studied to reveal normal and abnormal brain function [178]. The extension of these techniques to other NTs would enable an in-depth understanding of neurotransmitter functions in the human brain at normal and altered levels. Thus, electrochemical sensors have progressed at a very fast pace and significant advancements in the NCs may boost research in the neuroscience field [179].

5. Conclusions and Future Perspectives

Research on NC-based sensors has grown exponentially in the last decade. The emergence of various advanced NCs, comprising hierarchical porous carbon, graphene-based 2D and 3D NCs, GQDs, CNTs, conducting polymers, MIPs, and MOFs, is currently attracting the interest of researchers. Owing to their fascinating properties, such as high surface area and excellent conductivity, many NCs have been scrutinized for developing electrochemical sensors for NTs measurements. NC-based electrochemical sensors are emerging as powerful candidates for future diagnostic applications, owing to their sensitivity and rapid estimation of NTs. In this review article, we discuss important NC-based electrochemical sensors for the detection of NTs, with the main emphasis on non-enzymatic detection principle.

Many recently published studies have reported improvements in NC-based sensors for sensitive detection. Many past studies have started with the use of nanomaterials, typically carbon-based nanomaterials. Currently, considerable research is focused on the integration of novel combinations of NCs to achieve outstanding analytical performance in sensors. However, the commercialization of these sensors is still a big challenge, as it warrants the selective estimation of NTs in various co-existing species. Therefore, the efforts contributed by various researchers have made significant improvements in the sensitivity of detection; however, more studies are still needed to identify selective sensing platforms.

Inevitably, fouling problems due to adsorption of proteins from the real samples prompt measurement challenges; therefore, the robustness and reproducibility of the sensors is needed. Despite the plentiful advantages of electrochemical sensors, their application toward NTs in human samples faces serious challenges in terms of biocompatibility and real-time continuous monitoring. These challenges can be effectively encountered by modifying the sensors with NCs with a high surface area and target-specific features that readily overcome fouling effects. Further developments in electrochemical sensors through the integration of the abovementioned modifications might help to revolutionize the diagnosis of NDs.

It is pertinent to mention here that much research has been focused on enzyme-based GLU and GABA biosensors, whereas only a limited number of electrochemical sensors for GLU and GABA have been reported, as they are non-redox-active. Additionally, the performance of the sensors toward NTs detection by applying lower applied potentials requires extensive research. The fulfillment of this research gap may contribute to the rapid and efficient diagnosis of NDs.

In the near future, the principal goal of electrochemical sensing applications will be the development of skin-like/biomimetic sensors for the real-time and continuous monitoring of NTs. To achieve this goal, new electrochemical techniques, such as fast scan cycling voltammetry, are being continuously explored for NTs monitoring. Additionally, implantable sensors with quick responses, electrode arrays that can simultaneously detect a panel of NTs (with effective calibration and computational methods), smartphone-based sensors, and skin-like biomimetic sensors, require extensive research. Further advancements have focused on the development of high-throughput miniaturized/portable sensor arrays incorporating NCs.

This review has compiled numerous articles published regarding electrochemical detection of NTs. In addition, the basic concept of using each NC for surface modification

is discussed in detail. This review will be helpful in opening new ideas for the selective detection of NTs through electrochemical techniques for clinical applications.

Author Contributions: Conceptualization, T.R., M.K. and S.-C.C.; writing—original draft, T.R.; writing—review and editing, T.R., M.K., S.H. and S.-C.C.; supervision, M.K. and S.-C.C.; funding acquisition, S.-C.C. All authors have read and agreed to the published version of the manuscript.

Funding: This research was supported by the Basic Science Research Program through the National Research Foundation of Korea (NRF) funded by the Ministry of Education (2022R1I1A3072535). This research was supported by Korea Institute for Advancement of Technology (KIAT) grant funded by the Korea Government (MOTIE) (P0008763, HRD Program for Industrial Innovation).

Institutional Review Board Statement: Not applicable.

Informed Consent Statement: Not applicable.

Data Availability Statement: Not applicable.

Acknowledgments: We thank Bo Sung Shin in Pusan National University for helpful financial support and discussions during this research.

Conflicts of Interest: The authors declare no conflict of interest.

References

1. Gao, Y.-L.; Wang, N.; Sun, F.-R.; Cao, X.-P.; Zhang, W.; Yu, J.-T. Tau in neurodegenerative disease. *Ann. Transl. Med.* **2018**, *6*, 175. [[CrossRef](#)] [[PubMed](#)]
2. Dichgans, J.; Schulz, J.B. Aging in parts? Systemic aging of the nervous system. *Nervenarzt* **1999**, *70*, 1072–1081. [[CrossRef](#)] [[PubMed](#)]
3. Sengupta, U.; Kaye, R. Amyloid β , Tau, and α -Synuclein aggregates in the pathogenesis, prognosis, and therapeutics for neurodegenerative diseases. *Prog. Neurobiol.* **2022**, *214*, 102270. [[CrossRef](#)] [[PubMed](#)]
4. Armstrong, R. What causes neurodegenerative disease? *Folia Neuropathol.* **2020**, *58*, 93–112. [[CrossRef](#)] [[PubMed](#)]
5. Kirwan, S.M.; Rochitta, G.; McMahon, C.P.; Craig, J.D.; Killiron, S.J.; O'Brien, K.B.; Serra, P.A.; Lowry, J.P.; O'Neill, R.D. Modifications of Poly(o-phenylenediamine) permselective layer on Pt-Ir for biosensor application in neurochemical monitoring. *Sensors* **2007**, *7*, 420–437. [[CrossRef](#)]
6. Zhang, J.; Liu, X.; Neri, G.; Pinna, N. Nanostructured materials for room-temperature gas sensors. *Adv. Mater.* **2016**, *28*, 795–831. [[CrossRef](#)]
7. Martin, W.R.W. MR spectroscopy in neurodegenerative disease. *Mol. Imaging Biol.* **2007**, *9*, 196–203. [[CrossRef](#)]
8. Bicker, J.; Fortuna, A.; Alves, G.; Falcao, A. Liquid chromatographic methods for the quantification of catecholamines and their metabolites in several biological samples—a review. *Anal. Chim. Acta* **2013**, *768*, 12–34. [[CrossRef](#)]
9. Cao, Q.; Wang, Y.; Chen, B.; Ma, F.; Hao, L.; Li, G.; Ouyang, C.; Li, L. Visualization and identification of neurotransmitters in crustacean brain via multifaceted mass spectrometric approaches. *ACS Chem. Neurosci.* **2019**, *10*, 1222–1229. [[CrossRef](#)]
10. Kennedy, R.T.; Watson, C.J.; Haskins, W.E.; Powell, D.H.; Strecker, R.E. In vivo neurochemical monitoring by microdialysis and capillary separations. *Curr. Opin. Chem. Biol.* **2002**, *6*, 659–665. [[CrossRef](#)]
11. Moukhles, H.; Bosler, O.; Bolam, J.P.; Vallee, A.; Umbriaco, D.; Geffard, M.; Doucet, G. Quantitative and morphometric data indicate precise cellular interactions between serotonin terminals and postsynaptic targets in rat substantia nigra. *Neuroscience* **1997**, *76*, 1159–1171. [[CrossRef](#)] [[PubMed](#)]
12. Xiong, J.; Yang, Y.; Wang, L.; Chen, S.; Du, Y.; Song, Y. Electrochemical sensors based on metal-porous carbon nanozymes for dopamine, uric acid and furazolidone. *Chemosensors* **2022**, *10*, 458. [[CrossRef](#)]
13. Shen, M.; Colombo, M.L. Electrochemical nanoprobe for the chemical detection of neurotransmitters. *Anal. Methods* **2015**, *7*, 7095–7105. [[CrossRef](#)] [[PubMed](#)]
14. Li, H.; Guo, C.-Y.; Xu, C.-L. A highly sensitive non-enzymatic glucose sensor based on bimetallic Cu-Ag superstructures. *Biosens. Bioelectron.* **2015**, *63*, 339–346. [[CrossRef](#)] [[PubMed](#)]
15. Batra, B.; Kumari, S.; Pundir, C.S. Construction of glutamate biosensor based on covalent immobilization of glutamate oxidase on polypyrrole nanoparticles/polyaniline modified gold electrode. *Enzyme Microb. Technol.* **2014**, *57*, 69–77. [[CrossRef](#)]
16. Available online: https://pubmed.ncbi.nlm.nih.gov/?term=nanocomposite+based+electrochemical+sensors&filter=datesearch.y_5 (accessed on 18 January 2023).
17. Liu, X.; Ma, T.; Pinna, N.; Zhang, J. Two-dimensional nanostructured materials for gas sensing. *Adv. Funct. Mater.* **2017**, *27*, 1702168. [[CrossRef](#)]
18. Joshi, N.; Hayasaka, T.; Liu, Y.; Liu, H.; Olivera, O.N.; Lin, L. A review on chemiresistive room temperature gas sensors based on metal oxide nanostructures, graphene and 2D transition metal dichalcogenides. *Microchim. Acta* **2018**, *185*, 213. [[CrossRef](#)]

19. Thanh, T.D.; Balamurugan, J.; Lee, S.H.; Kim, N.H.; Lee, J.H. Novel porous gold-palladium nanoalloy network-supported graphene as an advanced catalyst for non-enzymatic hydrogen peroxide sensing. *Biosens. Bioelectron.* **2016**, *85*, 669–678. [CrossRef]
20. Yang, P.; Tong, X.; Wang, G.; Gao, Z.; Guo, X.; Qin, Y. NiO/SiC nanocomposite prepared by atomic layer deposition used as a novel electrocatalyst for nonenzymatic glucose sensing. *ACS Appl. Mater. Interfaces* **2015**, *7*, 4772–4777. [CrossRef]
21. Goldstein, D.S.; Sullivan, P.; Holmes, C.; Mash, D.C.; Kopin, I.J.; Sharabi, Y. Determinants of denervation-independent depletion of putamen dopamine in Parkinson's disease and multiple system atrophy. *Park. Relat. Disord.* **2017**, *35*, 88–91. [CrossRef]
22. Kleppner, S.R.; Tobin, A.J. GABA signalling: Therapeutic targets for epilepsy, Parkinson's disease and Huntington's disease. *Expert Opin. Ther. Targets* **2001**, *5*, 219–239. [CrossRef] [PubMed]
23. Wu, K.; Fei, J.; Hu, S. Simultaneous determination of dopamine and serotonin on a glassy carbon electrode coated with a film of carbon nanotubes. *Anal. Biochem.* **2003**, *318*, 100–106. [CrossRef] [PubMed]
24. Eulenburg, V.; Gomeza, J. Neurotransmitter transporters expressed in glial cells as regulators of synapse function. *Brain Res. Rev.* **2010**, *63*, 103–112. [CrossRef] [PubMed]
25. Hinzman, J.M.; Thomas, T.C.; Burmeister, J.J.; Quintero, J.E.; Huettl, P.; Pomerleau, F.; Gerhardt, G.A.; Lifshitz, J. Diffuse brain injury elevates tonic glutamate levels and potassium-evoked glutamate release in discrete brain regions at two days post-injury: An enzyme-based microelectrode array study. *J. Neurotrauma* **2010**, *27*, 889–899. [CrossRef]
26. Parsons, M.P.; Raymond, L.A. Extrasynaptic NMDA receptor involvement in central nervous system disorders. *Neuron* **2014**, *82*, 279–293. [CrossRef]
27. Baluta, S.; Malecha, K.; Swist, A.; Cabaj, J. Fluorescence sensing platforms for epinephrine detection based on low temperature cofired ceramics. *Sensors* **2020**, *20*, 1429. [CrossRef]
28. Mazloum-Ardakani, M.; Beitollahi, H.; Mohseni, M.A.S.; Benvidi, A.; Naeimi, H.; Nejati-Barzoki, M.; Taghavinia, N. Simultaneous determination of epinephrine and acetaminophen concentrations using a novel carbon paste electrode prepared with 2,2'-[1,2 butanediylbis(nitriloethylidene)]-bis-hydroquinone and TiO₂ nanoparticles. *Colloids Surf. B Biointerfaces* **2010**, *76*, 82–87. [CrossRef]
29. Available online: <https://www.myupchar.com/en/test/catecholamines-blood> (accessed on 18 January 2023).
30. Kumata, H.; Nishimura, R.; Nakanishi, C.; Inoue, C.; Tezuka, Y.; Endo, H.; Miyagi, S.; Tominaga, T.; Unno, M.; Kamei, T. Surgical strategy for an adult patient with a catecholamine-producing ganglioneuroblastoma and a cerebral aneurysm: A case report. *Surg. Case Rep.* **2018**, *4*, 119. [CrossRef]
31. Hsine, Z.; Mlika, R.; Jaffrezic-Renault, N.; Korri-Youssofi, H. Review—Recent progress in graphene based modified electrodes for electrochemical detection of dopamine. *Chemosensors* **2022**, *10*, 249. [CrossRef]
32. Wang, S.; Guo, P.; Ma, G.; Wei, J.; Wang, Z.; Cui, L.; Sun, L.; Wang, A. Three-dimensional hierarchical mesoporous carbon for regenerative electrochemical dopamine sensor. *Electrochim. Acta* **2020**, *360*, 137016. [CrossRef]
33. Dong, L.; Fan, L.; Yigang, D. Hierarchical porous carbon derived from pyrolysis of sodium citrate for sensitive determination of dopamine and uric acid. *J. Electrochem. Soc.* **2019**, *166*, B1585–B1593. [CrossRef]
34. Liu, S.; Gao, S.; Fei, T.; Zhang, T. Highly sensitive and selective dopamine detection utilizing nitrogen-doped mesoporous carbon prepared by a molten glucose-assisted hard-template approach. *Chempluschem* **2019**, *84*, 845–852. [CrossRef] [PubMed]
35. Sui, Z.-Y.; Meng, Y.-N.; Xiao, P.-W.; Zhao, Z.-Q.; Wei, Z.-X.; Han, B.-H. Nitrogen-doped graphene aerogels as efficient supercapacitor electrodes and gas adsorbents. *ACS Appl. Mater. Interfaces* **2015**, *7*, 1431–1438. [CrossRef] [PubMed]
36. Ding, A.; Wang, B.; Zheng, J.; Weng, B.; Li, C. Sensitive dopamine sensor based on three dimensional and macroporous carbon aerogel microelectrode. *Int. J. Electrochem. Sci.* **2018**, *13*, 4379–4389. [CrossRef]
37. Vilian, A.T.E.; An, S.; Choe, S.R.; Kwak, C.H.; Huh, Y.S.; Lee, J.; Han, Y.-K. Fabrication of 3D honeycomb-like porous polyurethane-functionalized reduced graphene oxide for detection of dopamine. *Biosens. Bioelectron.* **2016**, *86*, 122–128. [CrossRef]
38. Keisham, B.; Seksenyan, A.; Denyer, S.; Kheirkhah, P.; Arnone, G.D.; Avalos, P.; Bhimani, A.D.; Svendsen, C.; Berry, V.; Mehta, A.I. Quantum capacitance based amplified graphene phononics for studying neurodegenerative diseases. *ACS Appl. Mater. Interfaces* **2019**, *11*, 169–175. [CrossRef]
39. Suriyaparakash, J.; Bala, K.; Shan, L.; Wu, L.; Gupta, N. Molecular engineered carbon-based sensor for ultrafast and specific detection of neurotransmitters. *ACS Appl. Mater. Interfaces* **2021**, *13*, 60878–60893. [CrossRef]
40. Liu, X.-P.; Tong, J.; Yuan, Z.; Yang, Y.; Mao, C.-J.; Niu, H.-L.; Jin, B.-K.; Zhang, S.-Y. Highly sensitive electrochemical dopamine sensor from poly(diallyldimethylammonium chloride)-functionalized graphene nanoribbon/gold nanoparticle nanocomposite. *J. Nanosci. Nanotechnol.* **2016**, *16*, 1645–1649. [CrossRef]
41. Mohanan, V.M.A.; Kunnummal, A.K.; Biju, V.M.N. Selective electrochemical detection of dopamine based on molecularly imprinted poly(5-amino 8-hydroxy quinoline) immobilized reduced graphene oxide. *J. Mater. Sci.* **2018**, *53*, 10627–10639. [CrossRef]
42. Gao, F.; Cai, X.; Wang, X.; Gao, C.; Liu, S.; Gao, F.; Wang, Q. Highly sensitive and selective detection of dopamine in the presence of ascorbic acid at graphene oxide modified electrode. *Sens. Actuators B Chem.* **2013**, *186*, 380–387. [CrossRef]
43. Chu, K.; Wang, F.; Zhao, X.-L.; Wang, X.-W.; Tian, Y. Electrochemical dopamine sensor based on P-doped graphene: Highly active metal-free catalyst and metal catalyst support. *Mater. Sci. Eng. C* **2017**, *81*, 452–458. [CrossRef] [PubMed]
44. Ma, F.; Yang, B.; Zhang, Z.; Kong, J.; Huang, G.; Mei, Y. Self-rolled TiO₂ microscroll/graphene composite for electrochemical dopamine sensing. *Prog. Nat. Sci.* **2020**, *30*, 337–342. [CrossRef]

45. Tezerjani, M.D.; Benvidi, A.; Dehghani Firouzabadi, A.; Mazloun-Ardakani, M.; Akbari, A. Epinephrine electrochemical sensor based on a carbon paste electrode modified with hydroquinone derivative and graphene oxide nano-sheets: Simultaneous determination of epinephrine, acetaminophen and dopamine. *Measurement* **2017**, *101*, 183–189. [[CrossRef](#)]
46. Yadav, S.K.; Agrawal, B.; Oyama, M.; Goyal, R.N. Graphene modified palladium sensor for electrochemical analysis of norepinephrine in pharmaceuticals and biological fluids. *Electrochim. Acta* **2014**, *125*, 622–629.
47. Ma, Y.; Han, J.; Tong, Z.; Qin, J.; Wang, M.; Suhr, J.; Nam, J.; Xiao, L.; Jia, S.; Chen, X. Porous carbon boosted non-enzymatic glutamate detection with ultra-high sensitivity in broad range using cu ions. *Nanomaterials* **2022**, *12*, 1987. [[CrossRef](#)]
48. Alamry, K.A.; Hussein, M.A.; Choi, J.-W.; El-Said, W.A. Non-enzymatic electrochemical sensor to detect γ -aminobutyric acid with ligand-based on graphene oxide modified gold electrode. *J. Electroanal. Chem.* **2020**, *879*, 114789. [[CrossRef](#)]
49. Nirala, N.R.; Abraham, S.; Kumar, V.; Bansal, A.; Srivastava, A.; Saxena, P.S. Colorimetric detection of cholesterol based on highly efficient peroxidase mimetic activity of graphene quantum dots. *Sens. Actuators B Chem.* **2015**, *218*, 42–50. [[CrossRef](#)]
50. Jang, H.-S.; Kim, D.; Lee, C.; Yan, B.; Qin, X.; Piao, Y. Nafion coated Au nanoparticle-graphene quantum dot nanocomposite modified working electrode for voltammetric determination of dopamine. *Inorg. Chem. Commun.* **2019**, *105*, 174–181. [[CrossRef](#)]
51. Pang, P.; Yan, F.; Li, H.; Li, H.; Zhang, Y.; Wang, H.; Wu, Z.; Yang, W. Graphene quantum dots and Nafion composite as an ultrasensitive electrochemical sensor for the detection of dopamine. *Anal. Methods* **2016**, *8*, 4912–4918. [[CrossRef](#)]
52. Luhana, C.; Moyo, I.; Tshenkeng, K.; Mashazi, P. In-sera selectivity detection of catecholamine neurotransmitters using covalent composite of cobalt phthalocyanine and aminated graphene quantum dots. *Microchem. J.* **2022**, *180*, 107605. [[CrossRef](#)]
53. Huang, Q.; Lin, X.; Tong, L.; Tong, Q.-X. Graphene quantum dots/multiwalled carbon nanotubes composite-based electrochemical sensor for detecting dopamine release from living cells. *ACS Sustain. Chem. Eng.* **2020**, *8*, 1644–1650. [[CrossRef](#)]
54. Arumugasamy, S.K.; Govindaraju, S.; Yun, K. Electrochemical sensor for detecting dopamine using graphene quantum dots incorporated with multiwall carbon nanotubes. *Appl. Surf. Sci.* **2020**, *508*, 145294. [[CrossRef](#)]
55. Galal, A.; Atta, N.F.; El-Ads, E.H.; El-Gohary, A.R.M. Fabrication of β -cyclodextrin/glycine/carbon nanotubes electrochemical neurotransmitters sensor—Application in ultra-sensitive determination of DOPAC in human serum. *Electroanalysis* **2018**, *30*, 1678–1688. [[CrossRef](#)]
56. Lin, R.; Lim, T.M.; Tran, T. Carbon nanotube band electrodes for electrochemical sensors. *Electrochem. Commun.* **2018**, *86*, 135–139. [[CrossRef](#)]
57. Merkoçi, A.; Pumera, M.; Llopis, X.; Pérez, B.; del Valle, M.; Alegret, S. New materials for electrochemical sensing VI: Carbon nanotubes. *TrAC Trends Anal. Chem.* **2005**, *24*, 826–838. [[CrossRef](#)]
58. Chapin, A.A.; Rajasekaran, P.R.; Quan, D.N.; Hu, L.; Herberholz, J.; Bentley, W.E.; Ghodssi, R. Electrochemical measurement of serotonin by Au-CNT electrodes fabricated on microporous cell culture membranes. *Microsyst. Nanoeng.* **2020**, *6*, 90. [[CrossRef](#)]
59. Rajarathinam, T.; Thirumalai, D.; Kwon, M.; Lee, S.; Jayaraman, S.; Paik, H.-J.; Lee, J.; Chang, S.-C. Screen-printed carbon electrode modified with de-bundled single-walled carbon nanotubes for voltammetric determination of norepinephrine in ex vivo rat tissue. *Bioelectrochemistry* **2022**, *146*, 108155. [[CrossRef](#)]
60. Li, J.; Huang, X.; Shi, W.; Jiang, M.; Tian, L.; Su, M.; Wu, J.; Liu, Q.; Yu, C.; Gu, H. Pt nanoparticle decorated carbon nanotubes nanocomposite based sensing platform for the monitoring of cell-secreted dopamine. *Sens. Actuators B Chem.* **2021**, *330*, 129311. [[CrossRef](#)]
61. Vlckova, M.; Schwarz, M.A. Determination of cationic neurotransmitters and metabolites in brain homogenates by microchip electrophoresis and carbon nanotube-modified amperometry. *J. Chromatogr. A* **2007**, *1142*, 214–221. [[CrossRef](#)]
62. Mercante, L.A.; Pavinatto, A.; Iwaki, L.E.O.; Scagion, V.P.; Zucolotto, V.; Oliveira, O.N., Jr.; Mattoso, L.H.C.; Correa, D.S. Electrospun polyamide 6/poly(allylamine hydrochloride) nanofibers functionalized with carbon nanotubes for electrochemical detection of dopamine. *ACS Appl. Mater. Interfaces* **2015**, *7*, 4784–4790. [[CrossRef](#)]
63. Kumar, S.; Awasthi, A.; Sharma, M.D.; Singh, K.; Singh, D. Functionalized multiwall carbon nanotube-molybdenum disulphide nanocomposite based electrochemical ultrasensitive detection of neurotransmitter epinephrine. *Mater. Chem. Phys.* **2022**, *290*, 126656. [[CrossRef](#)]
64. Koteswara Reddy, K.; Satyanarayana, M.; Yugender Goud, K.; Vengatajalabathy Gobi, K.; Kim, H. Carbon nanotube ensembled hybrid nanocomposite electrode for direct electrochemical detection of epinephrine in pharmaceutical tablets and urine. *Mater. Sci. Eng. C* **2017**, *79*, 93–99. [[CrossRef](#)] [[PubMed](#)]
65. Atta, N.F.; Ahmed, Y.M.; Galal, A. Electrochemical determination of neurotransmitters at crown ether modified carbon nanotube composite: Application for sub-nano-sensing of serotonin in human serum. *Electroanalysis* **2018**, *31*, 1204–1214. [[CrossRef](#)]
66. Fagan-Murphy, A.; Patel, B.A. Compressed multiwall carbon nanotube composite electrodes provide enhanced electroanalytical performance for determination of serotonin. *Electrochim. Acta* **2014**, *138*, 392–399. [[CrossRef](#)]
67. Gorduk, O. Differential pulse voltammetric determination of serotonin using an acid-activated multiwalled carbon nanotube—Over-oxidized poly(3,4-ethylenedioxythiophene) modified pencil graphite electrode. *Anal. Lett.* **2019**, *53*, 1034–1052. [[CrossRef](#)]
68. Liu, Z.; Jin, M.; Cao, J.; Niu, R.; Li, P.; Zhou, G.; Yu, Y.; van den Berg, A.; Shui, L. Electrochemical sensor integrated microfluidic device for sensitive and simultaneous quantification of dopamine and 5-hydroxytryptamine. *Sens. Actuators B Chem.* **2018**, *273*, 873–883. [[CrossRef](#)]
69. Bonetto, M.C.; Muñoz, F.F.; Diz, V.E.; Sacco, N.J.; Cortón, E. Fused and unzipped carbon nanotubes, electrochemically treated, for selective determination of dopamine and serotonin. *Electrochim. Acta* **2018**, *283*, 338–348. [[CrossRef](#)]

70. Gupta, P.; Tsai, K.; Ruhunage, C.K.; Gupta, V.K.; Rahm, C.E.; Jiang, D.; Alvarez, N.T. True picomolar neurotransmitter sensor based on open-ended carbon nanotubes. *Anal. Chem.* **2020**, *92*, 8536–8545. [[CrossRef](#)]
71. Mendoza, A.; Asrat, T.; Liu, F.; Wonnemberg, P.; Zestos, A.G. Carbon nanotube yarn microelectrodes promote high temporal measurements of serotonin using fast scan cyclic voltammetry. *Sensors* **2020**, *20*, 1173. [[CrossRef](#)]
72. Clark, J.; Chen, Y.; Hinder, S.; Silva, S.R.P. Highly Sensitive Dopamine Detection Using a Bespoke Functionalised Carbon Nanotube Microelectrode Array. *Electroanalysis* **2017**, *29*, 2365–2376. [[CrossRef](#)]
73. Gerard, M.; Chaubey, A.; Malhotra, B.D. Application of conducting polymers to biosensors. *Biosens. Bioelectron.* **2002**, *17*, 345–359. [[CrossRef](#)] [[PubMed](#)]
74. Yang, C.; Liu, M.-M.; Bai, F.-Q.; Guo, Z.-Z.; Liu, H.; Zhong, G.-X.; Peng, H.-P.; Chen, W.; Lin, X.-H.; Lei, Y.; et al. An electrochemical biosensor for sensitive detection of nicotine-induced dopamine secreted by PC12 cells. *J. Electroanal. Chem.* **2019**, *832*, 217–224. [[CrossRef](#)]
75. Selvolini, G.; Lazzarini, C.; Marrazza, G. Electrochemical nanocomposite single-use sensor for dopamine detection. *Sensors* **2019**, *19*, 3097. [[CrossRef](#)] [[PubMed](#)]
76. Kolucaık, E.; Karabiberoglu, S.U.; Dursun, Z. Electrochemical determination of serotonin using pre-treated multi-walled carbon nanotube-polyaniline composite electrode. *Electroanalysis* **2018**, *30*, 2977–2987. [[CrossRef](#)]
77. Peairs, M.J.; Ross, A.E.; Venton, B.J. Comparison of Nafion- and overoxidized polypyrrole-carbon nanotube electrodes for neurotransmitter detection. *Anal. Methods* **2011**, *3*, 2379–2386. [[CrossRef](#)]
78. Kathiresan, V.; Thirumalai, D.; Rajarathinam, T.; Yeom, M.; Lee, J.; Kim, S.; Yoon, J.-H.; Chang, S.-C. A simple one-step electrochemical deposition of bioinspired nanocomposite for the non-enzymatic detection of dopamine. *J. Anal. Sci. Technol.* **2021**, *12*, 5. [[CrossRef](#)]
79. Ghanbari, K.; Bonyadi, S. An electrochemical sensor based on Pt nanoparticles decorated over-oxidized polypyrrole/reduced graphene oxide nanocomposite for simultaneous determination of two neurotransmitters dopamine and 5-Hydroxy tryptamine in the presence of ascorbic acid. *Int. J. Polym. Anal. Charact.* **2020**, *25*, 105–125. [[CrossRef](#)]
80. Ran, G.; Chen, X.; Xia, Y. Electrochemical detection of serotonin based on a poly(bromocresol green) film and Fe₃O₄ nanoparticles in a chitosan matrix. *RSC Adv.* **2017**, *7*, 1847–1851. [[CrossRef](#)]
81. Ran, G.; Chen, C.; Gu, C. Serotonin sensor based on a glassy carbon electrode modified with multiwalled carbon nanotubes, chitosan, and poly(p-aminobenzenesulfonate). *Microchim. Acta* **2015**, *182*, 1323–1328. [[CrossRef](#)]
82. Huang, J.; Xu, W.; Gong, Y.; Weng, S.; Lin, X. Selective and reliable electrochemical sensor based on Polythionine/AuNPs composites for epinephrine detection in serum. *Int. J. Electrochem. Sci.* **2016**, *11*, 8193–8203. [[CrossRef](#)]
83. Yan, X.; Lu, N.; Gu, Y.; Li, C.; Zhang, T.; Liu, H.; Zhang, Z.; Zhai, S. Catalytic activity of biomimetic model of cytochrome P450 in oxidation of dopamine. *Talanta* **2018**, *179*, 401–408. [[CrossRef](#)] [[PubMed](#)]
84. Thirumalai, D.; Lee, S.; Kwon, M.; Paik, H.J.; Lee, J.; Chang, S.-C. Disposable voltammetric sensor modified with block copolymer-dispersed graphene for simultaneous determination of dopamine and ascorbic acid in ex vivo mouse brain tissue. *Biosensors* **2021**, *11*, 368. [[CrossRef](#)] [[PubMed](#)]
85. da Silva, L.V.; Lopes, C.B.; da Silva, W.C.; de Paiva, Y.G.; dos Santos Silva, F.D.; Lima, P.R.; Kubota, L.T.; Goulart, M.O.F. Electropolymerization of ferulic acid on multi-walled carbon nanotubes modified glassy carbon electrode as a versatile platform for NADH, dopamine and epinephrine separate detection. *Microchem. J.* **2017**, *133*, 460–467. [[CrossRef](#)]
86. Sadanandhan, N.K.; Cheriyaathuchenaaramvalli, M.; Devaki, S.J.; Ravindranatha Menon, A.R. PEDOT-reduced graphene oxide-silver hybrid nanocomposite modified transducer for the detection of serotonin. *J. Electroanal. Chem.* **2017**, *794*, 244–253. [[CrossRef](#)]
87. da Silva, Q.G.; Vieira Barbosa, N.; de Pieri Troiani, E.; Censi Faria, R. Electrochemical determination of norepinephrine on cathodically pretreated Poly(1,5-diaminonaphthalene) modified electrode. *Electroanalysis* **2011**, *23*, 1359–1364. [[CrossRef](#)]
88. Vashist, S.K.; Zheng, D.; Al-Rubeaan, K.; Luong, J.H.T.; Sheu, F.-S. Advances in carbon nanotube based electrochemical sensors for bioanalytical applications. *Biotechnol. Adv.* **2011**, *29*, 169–188. [[CrossRef](#)]
89. Chen, P.-Y.; Vittal, R.; Nien, P.-C.; Ho, K.-C. Enhancing dopamine detection using a glassy carbon electrode modified with MWCNTs, quercetin, and Nafion[®]. *Biosens. Bioelectron.* **2009**, *24*, 3504–3509. [[CrossRef](#)]
90. Cui, F.; Zhou, Z.; Zhou, H.S. Molecularly imprinted polymers and surface imprinted polymers based electrochemical biosensor for infectious diseases. *Sensors* **2020**, *20*, 996. [[CrossRef](#)]
91. Morelli, I.; Chiono, V.; Vozzi, G.; Ciardelli, G.; Silvestri, D.; Giusti, P. Molecularly imprinted submicronspheres for applications in a novel model biosensor-film. *Sens. Actuators B Chem.* **2010**, *150*, 394–401. [[CrossRef](#)]
92. Song, W.; Chen, Y.; Xu, J.; Yang, X.-R.; Tian, D.-B. Dopamine sensor based on molecularly imprinted electrosynthesized polymers. *J. Solid State Electrochem.* **2010**, *14*, 1909–1914. [[CrossRef](#)]
93. Tertis, M.; Florea, A.; Adumitrachioaie, A.; Cernat, A.; Bogdan, D.; Barbu-Tudoran, L.; Jaffrezic Renault, N.; Sandulescu, R.; Cristea, C. Detection of dopamine by a biomimetic electrochemical sensor based on polythioaniline-bridged gold nanoparticles. *ChemPlusChem* **2017**, *82*, 561–569. [[CrossRef](#)] [[PubMed](#)]
94. Amatatongchai, M.; Sitanurak, J.; Sroysee, W.; Sodanant, S.; Chairam, S.; Jarujamrus, P.; Nacapricha, D.; Lieberzeit, P.A. Highly sensitive and selective electrochemical paper-based device using a graphite screen-printed electrode modified with molecularly imprinted polymers coated Fe₃O₄@Au@SiO₂ for serotonin determination. *Anal. Chim. Acta* **2019**, *1077*, 255–265. [[CrossRef](#)] [[PubMed](#)]

95. Furukawa, H.; Cordova, K.E.; O’Keeffe, M.; Yaghi, O.M. The chemistry and applications of metal-organic frameworks. *Science* **2013**, *341*, 1230444. [[CrossRef](#)] [[PubMed](#)]
96. Biswas, S.; Ahnfeldt, T.; Stock, N. New functionalized flexible Al-MIL-53-X (X = -Cl, -Br, -CH₃, -NO₂, -(OH)₂) solids: Syntheses, characterization, sorption, and breathing behavior. *Inorg. Chem.* **2011**, *50*, 9518–9526. [[CrossRef](#)]
97. Zhou, K.; Shen, D.; Li, X.; Chen, Y.; Hou, L.; Zhang, Y.; Sha, J. Molybdenum oxide-based metal-organic framework/polypyrrole nanocomposites for enhancing electrochemical detection of dopamine. *Talanta* **2020**, *209*, 120507. [[CrossRef](#)]
98. Moghzi, F.; Soleimannejad, J.; Sanudo, E.C.; Janczak, J. Dopamine sensing based on ultrathin fluorescent metal-organic nanosheets. *ACS Appl. Mater. Interfaces* **2020**, *12*, 44499–44507. [[CrossRef](#)]
99. Chen, S.S.; Han, P.-C.; Kuok, W.-K.; Lu, J.-Y.; Gu, Y.; Ahamad, T.; Alshehri, S.M.; Ayalew, H.; Yu, H.-H.; Wu, K.C.-W. Synthesis of MOF525/PEDOT composites as microelectrodes for electrochemical sensing of dopamine. *Polymers* **2020**, *12*, 1976. [[CrossRef](#)]
100. Yu, G.; Xia, J.; Zhang, F.; Wang, Z. Hierarchical and hybrid RGO/ZIF-8 nanocomposite as electrochemical sensor for ultrasensitive determination of dopamine. *J. Electroanal. Chem.* **2017**, *801*, 496–502. [[CrossRef](#)]
101. Ko, M.; Mendecki, L.; Eagleton, A.M.; Durbin, C.G.; Stolz, R.M.; Meng, Z.; Mirica, K.A. Employing conductive metal-organic frameworks for voltammetric detection of neurochemicals. *J. Am. Chem. Soc.* **2020**, *142*, 11717–11733. [[CrossRef](#)]
102. Xu, Y.; Zhu, T.; Niu, Y.; Ye, B.-C. Electrochemical detection of glutamate by metal-organic frameworks-derived Ni@NC electrocatalysts. *Microchem. J.* **2022**, *175*, 107229. [[CrossRef](#)]
103. Li, J.; Qu, J.; Yang, R.; Qu, L.; Harrington, P.B. A sensitive and selective electrochemical sensor based on Graphene quantum dot/gold nanoparticle nanocomposite modified electrode for the determination of quercetin in biological samples. *Electroanalysis* **2016**, *28*, 1322–1330. [[CrossRef](#)]
104. Sipuka, D.S.; Arotiba, O.A.; Sebokolodi, T.I.; Tsekeli, T.R.; Nkosi, D. Gold-dendrimer nanocomposite based electrochemical sensor for dopamine. *Electroanalysis* **2022**, *34*. [[CrossRef](#)]
105. Li, X.; Lu, X.; Kan, X. 3D electrochemical sensor based on poly(hydroquinone)/gold nanoparticles/nickel foam for dopamine sensitive detection. *J. Electroanal. Chem.* **2017**, *799*, 451–458. [[CrossRef](#)]
106. Tertiş, M.; Cernat, A.; Lacatiş, D.; Florea, A.; Bogdan, D.; Suci, M.; Săndulescu, R.; Cristea, C. Highly selective electrochemical detection of serotonin on polypyrrole and gold nanoparticles-based 3D architecture. *Electrochem. Commun.* **2017**, *75*, 43–47. [[CrossRef](#)]
107. Yang, Y.; Zeng, Y.; Tang, C.; Zhu, X.; Lu, X.; Liu, L.; Chen, Z.; Li, L. Voltammetric determination of 5-hydroxytryptamine based on the use of platinum nanoparticles coated with molecularly imprinted silica. *Microchim. Acta* **2018**, *185*, 219. [[CrossRef](#)]
108. Goyal, R.N.; Aziz, M.A.; Oyama, M.; Chatterjee, S.; Rana, A.R.S. Nanogold based electrochemical sensor for determination of norepinephrine in biological fluids. *Sens. Actuators B Chem.* **2011**, *153*, 232–238. [[CrossRef](#)]
109. Pitiphattharabun, S.; Meesombad, K.; Panomsuwan, G.; Jongprateep, O. MWCNT/Ti-doped ZnO nanocomposite as electrochemical sensor for detecting glutamate and ascorbic acid. *Int. J. Appl. Ceram. Technol.* **2021**, *19*, 467–479. [[CrossRef](#)]
110. Yang, Z.; Hu, G.; Chen, X.; Zhao, J.; Zhao, G. The nano-Au self-assembled glassy carbon electrode for selective determination of epinephrine in the presence of ascorbic acid. *Colloids Surf. B Biointerfaces* **2007**, *54*, 230–235. [[CrossRef](#)]
111. Wu, B.; Yeasmin, S.; Liu, Y.; Cheng, L.-J. Sensitive and selective electrochemical sensor for serotonin detection based on ferrocene-gold nanoparticles decorated multiwall carbon nanotubes. *Sens. Actuators B Chem.* **2022**, *354*, 131216. [[CrossRef](#)]
112. da Silva, V.N.C.; Farias, E.A.O.; Araujo, A.R.; Xavier Magalhaes, F.E.; Neves Fernandes, J.R.; Teles Souza, J.M.; Eiras, C.; da Silva, D.A.; do Vale Bastos, V.H.; Teixeira, S.S. Rapid and selective detection of dopamine in human serum using an electrochemical sensor based on zinc oxide nanoparticles, nickel phthalocyanines, and carbon nanotubes. *Biosens. Bioelectron.* **2022**, *210*, 114211. [[CrossRef](#)]
113. Truță, F.; Tertis, M.; Cristea, C.; Graur, F. Simultaneous detection of dopamine and serotonin in real complex matrices. *Curr. Anal. Chem.* **2021**, *17*, 374–384. [[CrossRef](#)]
114. Figueiredo-Filho, L.C.S.; Silva, T.A.; Vicentini, F.C.; Fatibello-Filho, O. Simultaneous voltammetric determination of dopamine and epinephrine in human body fluid samples using a glassy carbon electrode modified with nickel oxide nanoparticles and carbon nanotubes within a dihexadecylphosphate film. *Analyst* **2014**, *139*, 2842–2849. [[CrossRef](#)] [[PubMed](#)]
115. Emran, M.Y.; Shenashen, M.A.; Mekawy, M.; Azzam, A.M.; Akhtar, N.; Gomaa, H.; Selim, M.M.; Faheem, A.; El-Safty, S.A. Ultrasensitive in-vitro monitoring of monoamine neurotransmitters from dopaminergic cells. *Sens. Actuators B Chem.* **2018**, *259*, 114–124. [[CrossRef](#)]
116. Sun, D.; Li, H.; Li, M.; Li, C.; Dai, H.; Sun, D.; Yang, B. Electrodeposition synthesis of a NiO/CNT/PEDOT composite for simultaneous detection of dopamine, serotonin, and tryptophan. *Sens. Actuators B Chem.* **2018**, *259*, 433–442. [[CrossRef](#)]
117. Ghanbari, K.; Moloudi, M. Flower-like ZnO decorated polyaniline/reduced graphene oxide nanocomposites for simultaneous determination of dopamine and uric acid. *Anal. Biochem.* **2016**, *512*, 91–102. [[CrossRef](#)]
118. Wang, Y.; Wang, S.; Tao, L.; Min, Q.; Xiang, J.; Wang, Q.; Xie, J.; Yue, Y.; Wu, S.; Li, X.; et al. A disposable electrochemical sensor for simultaneous determination of norepinephrine and serotonin in rat cerebrospinal fluid based on MWNTs-ZnO/chitosan composites modified screen-printed electrode. *Biosens. Bioelectron.* **2015**, *65*, 31–38. [[CrossRef](#)]
119. Mphuthi, N.G.; Adekunle, A.S.; Ebenso, E.E. Electrocatalytic oxidation of epinephrine and norepinephrine at metal oxide doped phthalocyanine/MWCNT composite sensor. *Sci. Rep.* **2016**, *6*, 26938. [[CrossRef](#)]
120. Jamal, M.; Hasan, M.; Mathewson, A.; Razeeb, K.M. Disposable sensor based on enzyme-free Ni nanowire array electrode to detect glutamate. *Biosens. Bioelectron.* **2013**, *40*, 213–218. [[CrossRef](#)]

121. Samdani, K.J.; Samdani, J.S.; Kim, N.H.; Lee, J.H. FeMoO₄ based, enzyme-free electrochemical biosensor for ultrasensitive detection of norepinephrine. *Biosens. Bioelectron.* **2016**, *81*, 445–453. [[CrossRef](#)]
122. Paramparambath, S.; Shafath, S.; Maurya, M.R.; Cabibihan, J.-J.; Al-Ali, A.; Malik, R.A.; Sadasivuni, K.K. Nonenzymatic electrochemical sensor based on CuO-MgO composite for dopamine detection. *IEEE Sens. J.* **2021**, *21*, 25597–25605. [[CrossRef](#)]
123. Zhong, Z.; Wang, J.; Jiang, S.; Li, M.; Lin, J.; Pan, J.; Tao, X.; Xie, A.; Luo, S. Novel electrochemical sensor based on Fe₃O₄-ZrO₂-graphene oxide for determination of dopamine. *Ionics* **2022**, *28*, 4853–4865. [[CrossRef](#)]
124. Kokulnathan, T.; Joseph Anthuvan, A.; Chen, S.-M.; Chinnuswamy, V.; Kadirvelu, K. Trace level electrochemical determination of the neurotransmitter dopamine in biological samples based on iron oxide nanoparticle decorated graphene sheets. *Inorg. Chem. Front.* **2018**, *5*, 705–718. [[CrossRef](#)]
125. Vinay, M.M.; Arthoba Nayaka, Y. Iron oxide (Fe₂O₃) nanoparticles modified carbon paste electrode as an advanced material for electrochemical investigation of paracetamol and dopamine. *J. Sci. Adv. Mater. Devices* **2019**, *4*, 442–450. [[CrossRef](#)]
126. Nehru, L.; Chinnathambi, S.; Fazio, E.; Neri, F.; Leonardi, S.G.; Bonavita, A.; Neri, G. Electrochemical sensing of serotonin by a modified MnO(2)-graphene electrode. *Biosensors* **2020**, *10*, 33. [[CrossRef](#)]
127. Tomé, L.I.N.; Brett, C.M.A. Polymer/iron oxide nanoparticle modified glassy carbon electrodes for the enhanced detection of epinephrine. *Electroanalysis* **2019**, *31*, 704–710. [[CrossRef](#)]
128. Mazloum-Ardakani, M.; Maleki, M.; Khoshroo, A. High-performance electrochemical sensor based on electrodeposited iron oxide nanoparticle: Catecholamine as analytical probe. *J. Iran. Chem. Soc.* **2017**, *14*, 1659–1664. [[CrossRef](#)]
129. Shahzad, F.; Iqbal, A.; Zaidi, S.A.; Hwang, S.-W.; Koo, C.M. Nafion-stabilized two-dimensional transition metal carbide (Ti₃C₂T_x MXene) as a high-performance electrochemical sensor for neurotransmitter. *J. Ind. Eng. Chem.* **2019**, *79*, 338–344. [[CrossRef](#)]
130. Ni, M.; Chen, J.; Wang, C.; Wang, Y.; Huang, L.; Xiong, W.; Zhao, P.; Xie, Y.; Fei, J. A high-sensitive dopamine electrochemical sensor based on multilayer Ti₃C₂ MXene, graphitized multi-walled carbon nanotubes and ZnO nanospheres. *Microchem. J.* **2022**, *178*, 107410. [[CrossRef](#)]
131. Boobphahom, S.; Siripongpreda, T.; Zhang, D.; Qin, J.; Rattanawaleedirojn, P.; Rodthongkum, N. TiO₂/MXene-PVA/GO hydrogel-based electrochemical sensor for neurological disorder screening via urinary norepinephrine detection. *Microchim. Acta* **2021**, *188*, 387. [[CrossRef](#)]
132. Samdani, K.J.; Joh, D.W.; Rath, M.K.; Lee, K.T. Electrochemical mediatorless detection of norepinephrine based on MoO₃ nanowires. *Electrochim. Acta* **2017**, *252*, 268–274. [[CrossRef](#)]
133. Huang, K.-J.; Liu, Y.-J.; Liu, Y.-M.; Wang, L.-L. Molybdenum disulfide nanoflower-chitosan-Au nanoparticles composites based electrochemical sensing platform for bisphenol A determination. *J. Hazard. Mater.* **2014**, *276*, 207–215. [[CrossRef](#)] [[PubMed](#)]
134. Vijayaraj, K.; Dinakaran, T.; Lee, Y.; Kim, S.; Kim, H.S.; Lee, J.; Chang, S.-C. One-step construction of a molybdenum disulfide/multi-walled carbon nanotubes/polypyrrole nanocomposite biosensor for the ex-vivo detection of dopamine in mouse brain tissue. *Biochem. Biophys. Res. Commun.* **2017**, *494*, 181–187. [[CrossRef](#)] [[PubMed](#)]
135. Pramoda, K.; Moses, K.; Maitra, U.; Rao, C.N.R. Superior performance of a MoS₂-RGO composite and a borocarbonitride in the electrochemical detection of dopamine, uric acid, and adenine. *Electroanalysis* **2015**, *27*, 1892–1898. [[CrossRef](#)]
136. Balu, S.; Palanisamy, S.; Velusamy, V.; Yang, T.C.K.; El-Shafey, E.I. Tin disulfide nanorod-graphene-beta-cyclodextrin nanocomposites for sensing dopamine in rat brains and human blood serum. *Mater. Sci. Eng. C* **2020**, *108*, 110367. [[CrossRef](#)]
137. Sun, Y.; Fei, J.; Hou, J.; Zhang, Q.; Liu, Y.; Hu, B. Simultaneous determination of dopamine and serotonin using a carbon nanotubes-ionic liquid gel modified glassy carbon electrode. *Microchim. Acta* **2009**, *165*, 373–379. [[CrossRef](#)]
138. Liu, P.; Dong, M.; Lu, J.; Guo, H.; Lu, X.; Liu, X. Simultaneous determination of 5-hydroxytryptamine and dopamine using ionic liquid functionalized graphene. *Ionics* **2015**, *21*, 1111–1119. [[CrossRef](#)]
139. Li, Y.; Ji, Y.; Ren, B.; Jia, L.; Ma, G.; Liu, X. Carboxyl-functionalized mesoporous molecular sieve/colloidal gold modified nano-carbon ionic liquid paste electrode for electrochemical determination of serotonin. *Mater. Res. Bull.* **2019**, *109*, 240–245. [[CrossRef](#)]
140. Mazloum-Ardakani, M.; Khoshroo, A. High sensitive sensor based on functionalized carbon nanotube/ionic liquid nanocomposite for simultaneous determination of norepinephrine and serotonin. *J. Electroanal. Chem.* **2014**, 717–718, 17–23. [[CrossRef](#)]
141. Umaphathi, S.; Masud, J.; Coleman, H.; Nath, M. Electrochemical sensor based on CuSe for determination of dopamine. *Microchim. Acta* **2020**, *187*, 440. [[CrossRef](#)]
142. Pramanik, S.; Kumar, Y.; Karmakar, P.; Das, D.K. Nanosized Gadoliniumorthoferrite-based electrochemical sensor for the determination of dopamine. *Nano LIFE* **2021**, *11*, 3. [[CrossRef](#)]
143. Yan, X.; Gu, Y.; Li, C.; Zheng, B.; Li, Y.; Zhang, T.; Zhang, Z.; Yang, M. Morphology-controlled synthesis of Bi₂S₃ nanorods-reduced graphene oxide composites with high-performance for electrochemical detection of dopamine. *Sens. Actuators B Chem.* **2018**, *257*, 936–943. [[CrossRef](#)]
144. Ramachandran, A.; Panda, S.; Karunakaran Yesodha, S. Physiological level and selective electrochemical sensing of dopamine by a solution processable graphene and its enhanced sensing property in general. *Sens. Actuators B Chem.* **2018**, *256*, 488–497. [[CrossRef](#)]
145. Thanh, T.D.; Balamurugan, J.; Hien, H.V.; Kim, N.H.; Lee, J.H. A novel sensitive sensor for serotonin based on high-quality of AuAg nanoalloy encapsulated graphene electrocatalyst. *Biosens. Bioelectron.* **2017**, *96*, 186–193. [[CrossRef](#)] [[PubMed](#)]
146. Manbohi, A.; Ahmadi, S.H. Sensitive and selective detection of dopamine using electrochemical microfluidic paper-based analytical nanosensor. *Sens. Bio-Sens. Res.* **2019**, *23*, 100270. [[CrossRef](#)]

147. Zhao, J.; Liu, H.; Yu, Z.; Quhe, R.; Zhou, S.; Wang, Y.; Liu, C.C.; Zhong, H.; Han, N.; Lu, J.; et al. Rise of silicene: A competitive 2D material. *Prog. Mater. Sci.* **2016**, *83*, 24–151. [[CrossRef](#)]
148. Krishnamoorthy, K.; Pazhamalai, P.; Kim, S.-J. Two-dimensional siloxene nanosheets: Novel high-performance supercapacitor electrode materials. *Energy Environ. Sci.* **2018**, *11*, 1595–1602. [[CrossRef](#)]
149. Parra, V.; Arrieta, Á.A.; Fernández-Escudero, J.A.; García, H.; Apetrei, C.; Rodríguez-Méndez, M.L.; de Saja, J.A. E-tongue based on a hybrid array of voltammetric sensors based on phthalocyanines, perylene derivatives and conducting polymers: Discrimination capability towards red wines elaborated with different varieties of grapes. *Sens. Actuators B Chem.* **2006**, *115*, 54–61. [[CrossRef](#)]
150. Diab, N.; Morales, D.M.; Andronescu, C.; Masoud, M.; Schuhmann, W. A sensitive and selective graphene/cobalt tetrasulfonated phthalocyanine sensor for detection of dopamine. *Sens. Actuators B Chem.* **2019**, *285*, 17–23. [[CrossRef](#)]
151. Uwaya, G.E.; Fayemi, O.E. Electrochemical detection of serotonin in banana at green mediated PPy/Fe₃O₄NPs nanocomposites modified electrodes. *Sens. Bio-Sens. Res.* **2020**, *28*, 100338. [[CrossRef](#)]
152. Ramos, M.M.V.; Carvalho, J.H.S.; de Oliveira, P.R.; Janegitz, B.C. Determination of serotonin by using a thin film containing graphite, nanodiamonds and gold nanoparticles anchored in casein. *Measurement* **2020**, *149*, 106979. [[CrossRef](#)]
153. Babaei, A.; Taheri, A.R. Nafion/Ni(OH)₂ nanoparticles-carbon nanotube composite modified glassy carbon electrode as a sensor for simultaneous determination of dopamine and serotonin in the presence of ascorbic acid. *Sens. Actuators B Chem.* **2013**, *176*, 543–551. [[CrossRef](#)]
154. Sivasubramanian, R.; Biji, P. Preparation of copper (I) oxide nanohexagon decorated reduced graphene oxide nanocomposite and its application in electrochemical sensing of dopamine. *Mater. Sci. Eng. B* **2016**, *210*, 10–18. [[CrossRef](#)]
155. Ghoreishi, S.M.; Behpour, M.; Mortazavi, M.; Khoobi, A. Fabrication of a graphene oxide nano-sheet modified electrode for determination of dopamine in the presence of tyrosine: A multivariate optimization strategy. *J. Mol. Liq.* **2016**, *215*, 31–38. [[CrossRef](#)]
156. Hou, J.; Xu, C.; Zhao, D.; Zhou, J. Facile fabrication of hierarchical nanoporous AuAg alloy and its highly sensitive detection towards dopamine and uric acid. *Sens. Actuators B Chem.* **2016**, *225*, 241–248. [[CrossRef](#)]
157. Zhao, D.; Yu, G.; Tian, K.; Xu, C. A highly sensitive and stable electrochemical sensor for simultaneous detection towards ascorbic acid, dopamine, and uric acid based on the hierarchical nanoporous PtTi alloy. *Biosens. Bioelectron.* **2016**, *82*, 119–126. [[CrossRef](#)]
158. Liu, B.; Ouyang, X.; Ding, Y.; Luo, L.; Xu, D.; Ning, Y. Electrochemical preparation of nickel and copper oxides-decorated graphene composite for simultaneous determination of dopamine, acetaminophen and tryptophan. *Talanta* **2016**, *146*, 114–121. [[CrossRef](#)]
159. Han, H.S.; You, J.-M.; Jeong, H.; Jeon, S. Synthesis of graphene oxide grafted poly(lactic acid) with palladium nanoparticles and its application to serotonin sensing. *Appl. Surf. Sci.* **2013**, *284*, 438–445. [[CrossRef](#)]
160. Xue, C.; Wang, X.; Zhu, W.; Han, Q.; Zhu, C.; Hong, J.; Zhou, X.; Jiang, H. Electrochemical serotonin sensing interface based on double-layered membrane of reduced graphene oxide/polyaniline nanocomposites and molecularly imprinted polymers embedded with gold nanoparticles. *Sens. Actuators B Chem.* **2014**, *196*, 57–63. [[CrossRef](#)]
161. Dinesh, B.; Veeramani, V.; Chen, S.-M.; Saraswathi, R. In situ electrochemical synthesis of reduced graphene oxide-cobalt oxide nanocomposite modified electrode for selective sensing of depression biomarker in the presence of ascorbic acid and dopamine. *J. Electroanal. Chem.* **2017**, *786*, 169–176. [[CrossRef](#)]
162. Babaei, A.; Taheri, A.R.; Aminikhah, M. Nanomolar simultaneous determination of levodopa and serotonin at a novel carbon ionic liquid electrode modified with Co(OH)₂ nanoparticles and multi-walled carbon nanotubes. *Electrochim. Acta* **2013**, *90*, 317–325. [[CrossRef](#)]
163. Jamal, M.; Chakrabarty, S.; Shao, H.; McNulty, D.; Yousuf, M.A.; Furukawa, H.; Khosla, A.; Razeed, K.M. A non-enzymatic glutamate sensor based on nickel oxide nanoparticle. *Microsyst. Technol.* **2018**, *24*, 4217–4223. [[CrossRef](#)]
164. Hussain, M.M.; Rahman, M.M.; Asiri, A.M.; Awual, M.R. Non-enzymatic simultaneous detection of l-glutamic acid and uric acid using mesoporous Co₃O₄ nanosheets. *RSC Adv.* **2016**, *6*, 80511–80521. [[CrossRef](#)]
165. Ahmad, H.M.N.; Si, B.; Dutta, G.; Csoros, J.R.; Seitz, W.R.; Song, E. Non-enzymatic electrochemical detection of glutamate using templated polymer-based target receptors. In Proceedings of the 2019 20th International Conference on Solid-State Sensors, Actuators and Microsystems & Eurosensors XXXIII (TRANSDUCERS & EUROSENSORS XXXIII), Berlin, Germany, 23–27 June 2019; Volume 2019, pp. 613–616.
166. Zeynaloo, E.; Yang, Y.-P.; Dikici, E.; Landgraf, R.; Bachas, L.-G.; Daunert, S. Design of a mediator-free, non-enzymatic electrochemical biosensor for glutamate detection. *Nanomedicine* **2021**, *31*, 102305. [[CrossRef](#)] [[PubMed](#)]
167. Moraes, F.C.; Golinelli, D.L.C.; Mascaro, L.H.; Machado, S.A.S. Determination of epinephrine in urine using multi-walled carbon nanotube modified with cobalt phthalocyanine in a paraffin composite electrode. *Sens. Actuators B Chem.* **2010**, *148*, 492–497. [[CrossRef](#)]
168. Ma, X.; Chen, M.; Li, X.; Purushothaman, A.; Li, F. Electrochemical detection of norepinephrine in the presence of epinephrine, uric acid and ascorbic acid using a graphene-modified electrode. *Int. J. Electrochem. Sci.* **2012**, *7*, 991–1000.
169. Bian, C.; Zeng, Q.; Xiong, H.; Zhang, X.; Wang, S. Electrochemistry of norepinephrine on carbon-coated nickel magnetic nanoparticles modified electrode and analytical applications. *Bioelectrochemistry* **2010**, *79*, 1–5. [[CrossRef](#)] [[PubMed](#)]
170. Vilian, A.T.E.; Chen, S.-M.; Hung, Y.-T.; Ali, M.A.; Al-Hemaid, F.M.A. Electrochemical oxidation and determination of norepinephrine in the presence of acetaminophen using MnO₂ nanoparticle decorated reduced graphene oxide sheets. *Anal. Methods* **2014**, *6*, 6504–6513. [[CrossRef](#)]

171. Anandaraj, S.; Chen, T.-W.; Chen, S.-M.; Elaiyappillai, E.; Loganathan, S.; Ibrahimsa, S.L.; Johnson, P.M.; Selvin, P.S.; Weng, W.-H.; Leung, W.-H. Electrochemical detection of norepinephrine using sponge-like Co_3O_4 modified screen printed carbon electrode. *Int. J. Electrochem. Sci.* **2017**, *12*, 10524–10533. [[CrossRef](#)]
172. Wang, Z.; Wang, K.; Zhao, L.; Chai, S.; Zhang, J.; Zhang, X.; Zou, Q. A novel sensor made of Antimony doped Tin oxide-silica composite sol on a glassy carbon electrode modified by single-walled carbon nanotubes for detection of norepinephrine. *Mater. Sci. Eng. C* **2017**, *80*, 180–186. [[CrossRef](#)]
173. Hui, N.; Sun, X.; Niu, S.; Luo, X. PEGylated polyaniline nanofibers: Antifouling and conducting biomaterial for electrochemical DNA sensing. *ACS. Appl. Mater. Interfaces* **2017**, *9*, 2914–2923. [[CrossRef](#)]
174. Jackson, B.P.; Dietz, S.M.; Wightman, R.M. Fast-scan cyclic voltammetry of 5-hydroxytryptamine. *Anal. Chem.* **1995**, *67*, 1115–1120. [[CrossRef](#)] [[PubMed](#)]
175. Meunier, C.J.; McCarty, G.S.; Sombers, L.A. Drift subtraction for Fast-scan cyclic voltammetry using double-waveform partial-least-squares regression. *Anal. Chem.* **2019**, *91*, 7319–7327. [[CrossRef](#)] [[PubMed](#)]
176. Venton, B.J.; Cao, Q. Fundamentals of fast-scan cyclic voltammetry for dopamine detection. *Analyst* **2020**, *145*, 1158–1168. [[CrossRef](#)] [[PubMed](#)]
177. Jo, T.; Yoshimi, K.; Takahashi, T.; Oyama, G.; Hattori, N. Dual use of rectangular and triangular waveforms in voltammetry using a carbon fiber microelectrode to differentiate norepinephrine from dopamine. *J. Electroanal. Chem.* **2017**, *802*, 1–7. [[CrossRef](#)]
178. Park, C.; Oh, Y.; Shin, H.; Kim, J.; Kang, Y.; Sim, J.; Cho, H.U.; Lee, H.K.; Jung, S.J.; Blaha, C.D.; et al. Fast cyclic square-wave voltammetry to enhance neurotransmitter selectivity and sensitivity. *Anal. Chem.* **2018**, *90*, 13348–13355. [[CrossRef](#)]
179. Lucio Boschen, S.; Trevathan, J.; Hara, S.A.; Asp, A.; Lujan, J.L. Defining a path toward the use of Fast-scan cyclic voltammetry in human studies. *Front. Neurosci.* **2021**, *15*, 728092. [[CrossRef](#)]

Disclaimer/Publisher's Note: The statements, opinions and data contained in all publications are solely those of the individual author(s) and contributor(s) and not of MDPI and/or the editor(s). MDPI and/or the editor(s) disclaim responsibility for any injury to people or property resulting from any ideas, methods, instructions or products referred to in the content.